University of South-Eastern Norway

www.usn.no

FMH606 Master's Thesis 2023

Process Technology

MT-14-23

Design of Fine Powder Handling System Enhancing the Circularity of Aluminium Production

Source: HAL

Thanushi Rajinika Kumarawela

University of South-Eastern Norway

www.usn.no

Course: FMH606 Master's Thesis, 2023

Title: Design of Fine Powder Handling System Enhancing the Circularity of Aluminium Production

Number of pages: 78

Keywords: Alumina circular economy, pneumatic conveying, binary mixture, filter dust, basement dust, pressure drop

Student:	Thanushi Rajinika Kumarawela
Supervisor:	Chandana Ratnayake
External partner:	Serena Carmen Valciu, Chameera Jayarathna (Hydro Aluminium AS), Franz Otto von Hafenbrädl (SINTEF)

Summary:

Hydro Aluminium wants to separate fine powder particles (filter dust) from the process and send them to a specifically built storage silo by a pneumatic conveying line to mix with basement dust and feed back into the main silo. This approach will improve the circularity of the Aluminium manufacturing process; therefore, Hydro would like to investigate the preliminary design steps by analyzing the flow properties of the fine dust and how they may be controlled to develop a trouble-free and reliable handling system. The main objective of this study is to investigate fluidization properties and physical properties of pure particles and pressure drop calculations for given binary mixtures with different mass ratios of filter dust and basement dust and optimization of pressure drop calculations by varying the initial gas conditions while keeping the pipeline dimensions constant. The calculated U_{mf} and U_t values for pure particles based on selected mathematical models were found to be in pretty good line with the experimental values. The pressure drop calculation results show that the pressure drop is not affected by the mixture composition. It depends only on initial gas pressure and initial gas velocity. Initial velocities for all three mixtures can be set to a fixed value because the minimum conveying velocities and choking velocities are almost the same. To help in choosing the proper design parameters for a system it is required to perform pilot testing and validate the parameters.

Preface

This report was written in partial fulfillment of the Subject: FMH606 Master's Thesis requirement in Spring 2023. This is part of a project started by Hydro Aluminium in collaboration with the University of Southeast Norway and SINTEF to investigate the technical feasibility of pneumatic transportation of dust mixtures. The primary goal of this research is to investigate the fluidization and physical properties of dust particles to help in the early design phases. The report begins with a brief introduction to the project, objectives, and basic ideas of pneumatic conveying and fluidization, and then goes on to describe the theoretical calculations based on mathematical models and experimental work, as well as results and recommendations for future study.

First and foremost, I would want to express my sincere gratitude to my project supervisor, Chandana Ratnayake, who provided me with continual advice and support in completing this task. I'd also like to thank Serena Carmen Valciu, Chameera Jayarathna (Hydro Aluminium AS), and Franz Otto von Hafenbrädl (SINTEF) as project external partners for assisting me with laboratory work and providing valuable input from the industry when needed.

Porsgrunn, 12/05/2023

Thanushi Rajinika Kumarawela

Contents

List of Figures

List of Tables

Nomenclature

d_P = Particle diameter [m]

D = Pipeline inside diameter

f = Fanning friction factor

Fr_D = Frode number based on pipe diameter
$Fr_{fo}{}^*$ = pipe Frode number based on the terminal velocity of the particles
L = Equivalent length of pipeline

ΔP = Pressure drop [Pa]

ΔP_T = Total pressure drop in the system [Pa]

ΔP_{acc} = Pressure drop due to acceleration of the solids from their "at rest" condition at the pickup point to their conveying velocity up to their exit from the conveying system [Pa]

ΔP_a = Pressure drop of gas due to frictional losses between the gas and the pipe wall [Pa]

ΔP_s = Pressure drop of solids through the pipeline [Pa]

ΔH_a = Pressure drop due to elevation of gas in a vertical pipe [Pa]

ΔH_s = Pressure drop due to elevation of solids in a vertical pipe [Pa]

ΔP_{misc} = Pressure drop due to miscellaneous equipment [Pa]

$P_{45\mu m}$ = Weight fraction of particles <45 μm (fines content)

U_{mf} = Minimum fluidization velocity [cm/s]

U_{mb} = Minimum bubbling velocity [cm/s]

V_a = Air velocity [cm/s or m/s]

V_p = Particle velocity [cm/s or m/s]

W = Solids mass velocity, [kg/s·m^2]

ρ_a = air density [kg/m^3]

ρ_g = Gas density [kg/m^3]

μ = Gas viscosity [Ns/m^2]

$\emptyset_p$ = Particle sphericity

ε_{mf} = Minimum fluidization voidage

u_c = Superficial fluid velocity

λ_s = Additional pressure drop factor

μ = Solid loading ratio

1 Introduction

1.1 Background

Hydro Aluminium is a global leader in the production of Aluminium. Recently, extremely high dust exposure levels were detected in the anode rodding factory storage areas of one of Hydro's manufacturing units (Karmøy). To comply with company standards, it has been recommended that fine powder particles (filter dust) should be separated from the process and carried by a pneumatic conveyor to a specifically built storage silo, where they are mixed with basement dust and fed back into the main silo. In addition to concerns about health and safety, this approach will improve the circularity of the Aluminium manufacturing process. Hydro would like to investigate the preliminary design steps by analyzing the flow properties of the fine dust and how they may be controlled to develop a trouble-free and reliable handling system due to the high cost of retrofitting.

Hydro and SINTEF Tel-Tek have a long history of collaborating on powder technology knowledge development through research and development. SINTEF Tel-Tek has many bench and pilot-scale powder testing facilities. Hydro's Technology & Operational Support (TOS) Team in Porsgrunn has complementary powder flow testing facilities as well as an industrial knowledge base.

1.2 Aluminium production

In the Aluminium industry one of the main goals is to manufacture the end product, Aluminium metal, at lowest possible costs energy wise, while satisfying and maintaining product quality performance when it comes to raw materials (e.g., alumina). Environmental demands from the government and the public (stakeholders around the plants, e.g., farmers, households, and animals) enforce the need for an optimized design and a controlled interaction between the Aluminium production and raw material handling.

The study of the interaction and consequences between the Aluminium production and powder technology, represented by dusting has been inspired by the fact that handling of bulk solids is an essential element in the production of Aluminium metal and should be a key performance indicator (KPI).

1.2.1 Storage and conveying of Alumina at Aluminium plants

Approximately two tonnes of alumina are needed in order to produce one tonne of Aluminium. Thus, the storage silos must supply alumina at a rate of almost twice the Aluminium production. Main storage units used for alumina at the Aluminium smelters are silos with capacities equivalent to one or several shipments of alumina. For conveying the alumina over short to long distances (kilometers) from a quay to the potrooms or to the anode cover material plant, trucks, conveyor belts, pneumatic conveyors, air slides and other types are used . Downstream from the main primary alumina storage silos there are the fume treatment plants as shown in Figure 1, where both primary and secondary alumina (recycled, which previously had reacted

with the exhaust gas from the pots, HF and particulate fluoride) are used into the transport loop, up to six to seven times ((Dyroy, 2006), (Valciu, 2015)).

1.2.2 Distribution of Alumina to the electrolysis pots

Distribution of secondary alumina from the fume treatment plants to the pots is done by using front loaders driven from cell to cell, alumina being fed into small silos on the cells. Other plants use cranes. Pneumatic conveying systems are used by some others. During cooperation between Tel-Tek and the Technology Centre at Aardal Plant, a system based on air slides has been developed, the system being used in modern plants.

1.2.3 Feeding Alumina to electrolysis pots

Traditionally Alumina is fed to the pot by either volumetric or time-controlled dosing. During the process of making Aluminium, both secondary alumina and Aluminium fluoride are fed to the pot. Each pot has his own alumina and fluoride silos. The main parameters that one wishes to control are the dump weight sizes e.g., 850- 900 g, regarding dissolution, temperature, and power consumption in the pot. Thus, pots are fed with 900 g doses from each feeder, at a frequency given by the consumption of alumina, depending on the amperage for the electrolysis pot and the number of feeding points in the pot.

1.2.4 The electrolysis process

Aluminium metal is obtained from alumina by electrolytic reduction. The pots are connected in series to a direct current power source in the range of 280 - 450 kA. The pot contains a molten electrolyte, bath in which alumina from the feeders is dissolved. Additives like Aluminium fluoride needs to be used due to losses through evaporation. The emitted fluorides are collected and recycled to the pots through the secondary alumina in the fume treatment plants.

Suspended in the electrolyte are two parallel rows of anodes, acting as electrical conductors for the high intensity current. To prevent oxidation the anodes are covered by ACM using cranes. Each pot is kept closed by hoods to achieve greater scrubbing efficiency and ventilated in order to capture the emissions from the pot. Particulate emissions occur when the alumina is being introduced into the pots.

If there are too many fines in the fed material, they are captured and sucked out of the pot by the exhaust/ventilation system, or they come out into the working environment when the pots are opened during daily working operations. The same with the ACM covering the anodes, some of it goes to the potroom basement, through the floor gratings between the pots. Molten Aluminium is sucked from the bottom of the pot into large vehicles and transferred to the casting plant.

1.2.5 Dust generation in potrooms

Dust is fine particulate matter that escapes from process equipment during working operations and causes problems for the environment and humans. Fines are particles smaller than 45 μ m in the smelting environment, and they primarily consist of alumina or anode cover material

(ACM) (Hyland & Taylor, 2005). Such fines can cause issues in the process and most likely contribute to dust, either directly or indirectly. Many studies on the composition of potroom dust have been published (Hyland & Taylor, 2005). Alumina, electrolyte, carbon, and a variety of non-process specific elements such as rust, soil, and marine aerosols make up the majority of potroom dust. Fines are considered to have low dissolving rates and the process stability would be influenced by large or rapid variations in the alumina quality fed to the pot. Further, the frequency of working operations and control and deviation measurements needed to be carried out on a pot increases proportionally to the deviations in alumina and ACM quality fed to the potThe dust can form in a variety of ways according to the existing studies.

- Alumina spillage: alumina absorbs fluoride from the pot fume after passing through the dry-scrubbing system. This spillage occurs in the alumina transport systems that transfer the alumina to the cells (conveyors, bins, ore hoppers, etc.).
- Spillage of fine bath cover material (ACM), which is crushed to a size similar to fine alumina by some modern smelter bath crushing systems (supposedly to make it simpler to handle in dense phase lines). Bath components in potroom dust will be created from cell cover as crushed bath recovered from anode butts, in addition to condensed and entrained bath vapors associated with pot fume.
- Pot fume leakage from inside the cell cavity is produced by pot operation disturbances or procedures such as cell start-up, anode replacement, or bath tapping.
- Pot fume is a significant constituent of potroom dust. Together with the condensed bath, it will transport some alumina, anode cover, and carbon.

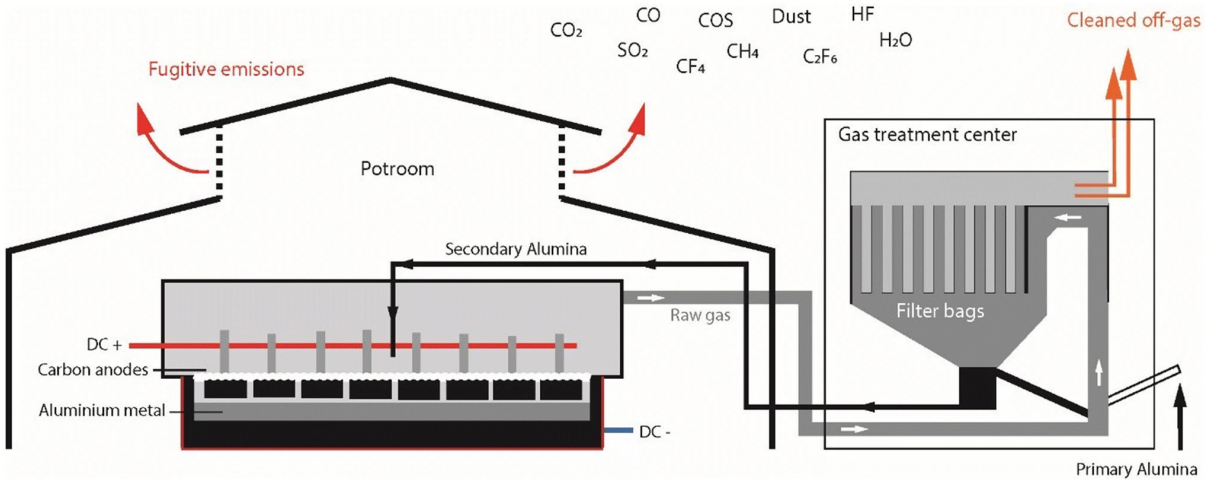

Figure 1.1 Schematic of the material flow of a potroom (Aarhaug & Ratvik, 2019)

Impurities are introduced into the anodes by recycled anode butts. These are largely bath components that were already in the cell, but they may also contain microscopic metallic pollutants from the earlier cleaning process. Typical dust loads in ducts have been observed to be in the range of 0.3 g dust per kg exhaust gas (Aarhaug & Ratvik, 2019). Based on research of contaminants in off-gas and secondary alumina, it is proven that the finer fractions are largely formed of condensed bath particles, whereas impurities are usually present in the lower micron-size fractions together with the secondary alumina fines. In this report, two types of dust are discussed. i.e.,

- Filter dust (Filterprøve): dust collected on the surface of the filter bags at the ACM plant
- Basement dust (Kjellerstøv): dust collected from the basement floor of the potroom

1.3 Objectives

Almost all processes in industry involve bulk solids and powders. Competition in the process industry forces companies to try to optimize the process and to reduce the environmental impact. This is not an easy task when some of the major input flow is a powder or bulk solid. The traditional way of handling bulk materials in industry has been conveying from A to B and storing into big bags, buckets, containers, or silos. Due to increased demands for low emissions of dust to the atmosphere from national authorities, industry is forced to increase focus on the handling of bulk materials. The main purpose of this project is to design a fine alumina powder handling system based on an experimental analysis of the powders' flow and transport characteristics. The study analyses the dust samples obtained from several locations at Hydro Aluminium's potroom and anode cover material (ACM) factory. Critical fine particle characteristics and fluidization properties should also be evaluated as part of the research. The published literature and commercially available fine powder handling solutions will be analyzed alongside the properties of the actual materials to draw conclusions and make necessary recommendations in the overall design of the fine particle handling system, and eventually, develop relevant circular economy routes of alumina and ACM handling processes. Further, once the points of needed improvements in the logistic loop of alumina and ACM are defined, proper actions must be implemented. These may be both implementation of proper handling equipment and change of existing standard operational procedures (SOPs).

2 Theoretical background

This chapter discusses background knowledge relevant to the experimental work performed in this research study. The experimental work is divided into three major categories: pneumatic conveying, particle fluidization, and particle flow characteristics.

2.1 Fluidization

The process of converting a stationary solid particle into a fluid-like condition by blowing a fluid through the particles is known as fluidization. As seen in Figure 2.1, the fluid is equally spread through a bed of solid particles.

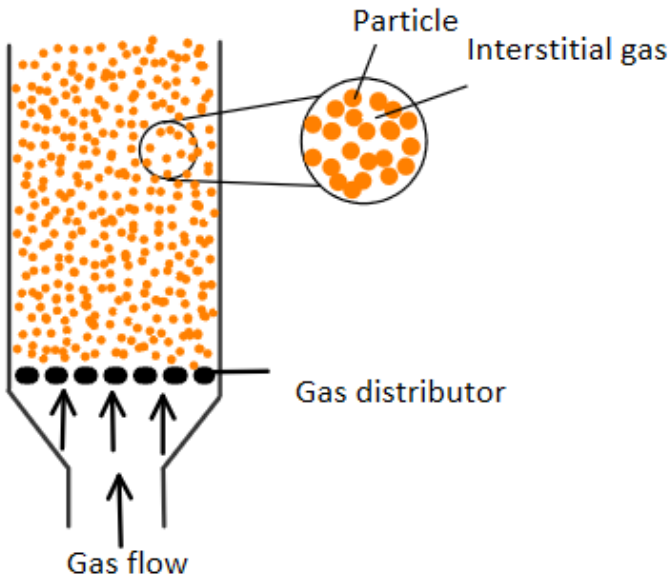

Figure 2.1 Fluidized bed reactor (Dechsiri, 2004)

At low fluid flow rates, when a fluid flows upwards through a bed of particles, the pressure drop over the bed is directly proportional to the fluid velocity. In this instance, the bed is considered a packed bed. When the gas velocity reaches a certain value (minimum fluidization velocity; U_{mf}) the particles start to move. The particles will be well mixed with one another and with the fluid (*MP-20-22*, 2022).

2.1.1 Fluidization regimes

Particles in a fluidization bed respond differently based on the gas flow rate, gas type, and particle properties. The various regimes seen in a fluidized bed are depicted in Figure 2.2.

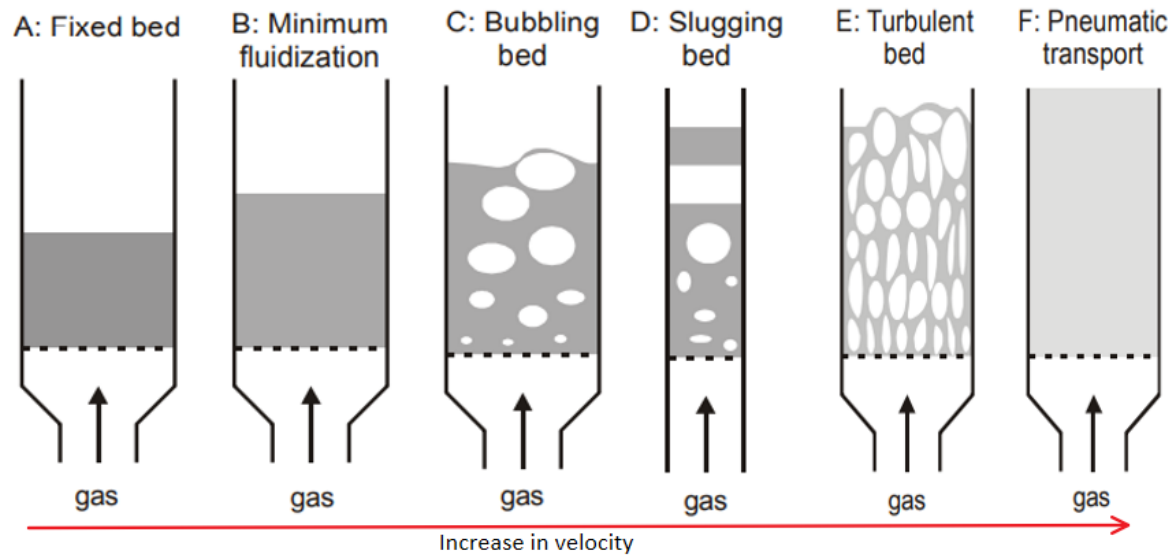

Figure 2.2 Fluidization regimes (Dechsiri, 2004)

- **A: Fixed bed**

As the flow of gas through a bed of particles is gradually increased, a few particles vibrate but remain at the same height as the bed at rest.

- **B: Minimum fluidization**

As the speed of gas flow increases, there comes a moment when the force of the gas pushing upwards balances the weight of the particles, causing the void fraction in the bed to increase slightly: the beginning of fluidization with a minimal fluidization velocity.

- **C: Bubbling bed**

Once the gas flow is increased further, the development of fluidization bubbles begins. A bubbling fluidized bed forms at this moment.

- **D: Slugging bed**

The bubbles in a bubbling fluidized bed will coalesce and develop as the velocity is increased. If the height-to-diameter ratio of the bed is high enough, the size of the bubbles may become the same as the diameter of the bed.

- **E: Turbulent flow**

If the particles are fluidized at a high enough gas flow rate, the velocity surpasses the particles' terminal velocity. Instead of bubbles, the upper surface of the bed vanishes, and a turbulent motion of solid clusters and voids of gas of various sizes and shapes is observed.

- **F: Pneumatic transport**

With further increases in gas velocity, the fluidized bed finally becomes an entrained bed in which is scattered, dilute, or lean phase fluidized bed, which equals pneumatic solid transport.

The flow regimes and transition from one regime to another depend on:

- Superficial gas velocity which is the operating gas velocity
- Bulk density of particles
- Fluid and particle characteristics: density, fluid viscosity, and particle size distribution

2.1.2 Classification of particles

The fluidization behavior of solid particles is strongly dependent on their characteristics given by mean particle sizes and density difference. Geldart sorted particles into four categories C, A, B, and D (Geldart, 1973) as shown in Figure 2.3.

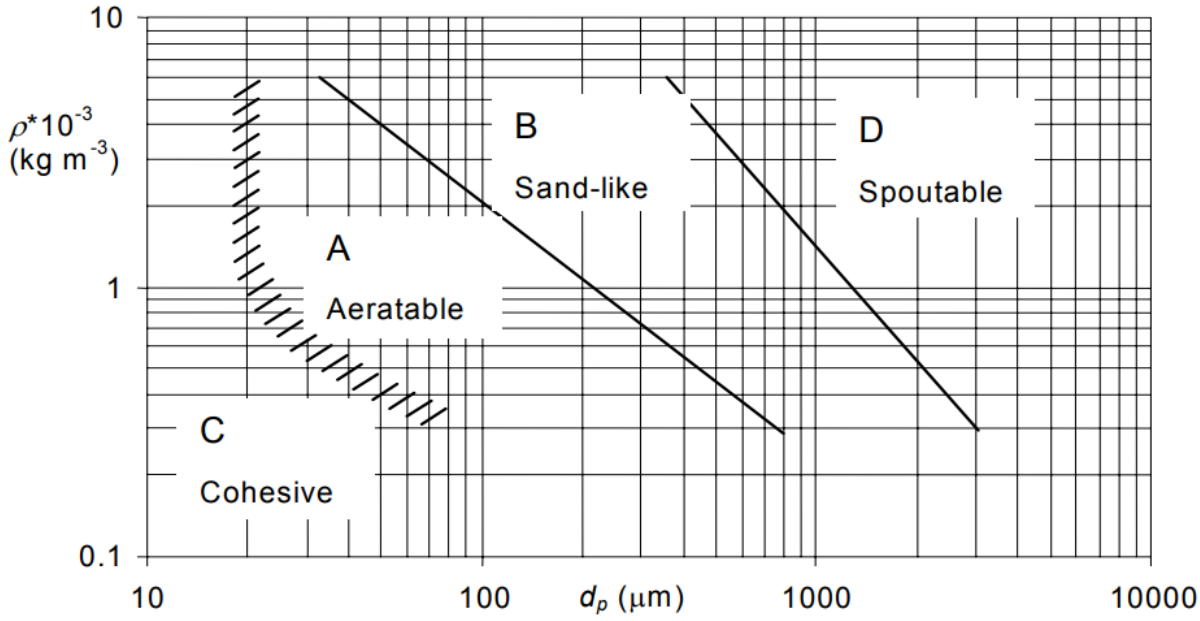

Figure 2.3 Geldart classification of particles (Geldart, 1973)

- **Group C**: very fine or cohesive particles. Particles in this region are difficult to fluidize due to strong inter-particle forces e.g., Vander Waals and electrostatics – which are greater than those exerted by the fluidized bed. Flour and starch are examples of materials that lie within this region.
- **Group A**: Particles in group A are easily fluidized with smooth fluidization at low gas velocities and controlled gas bubbles that break down at high velocities. With increasing the operating gas velocity in the bed, these particles start to fluidize and show bubbling after fluidizing.
- **Group B**: Sand-like particles that start fluidizing with intense bubbling due to the absence of inter-particle forces. Bubble size increases with increasing distance from the gas inlet.

- **Group D**: characterized by large particles with high density. Difficult to fluidize in deep beds and particles can be blown out in a spouting motion. Roasting coffee beans and lead shots are examples that lie within the group D region (Kunii & Levenspiel, 2012).

2.1.3 Minimum fluidization velocity

Minimum fluidization velocity is the superficial fluid velocity at which a bed of particles starts to fluidize.

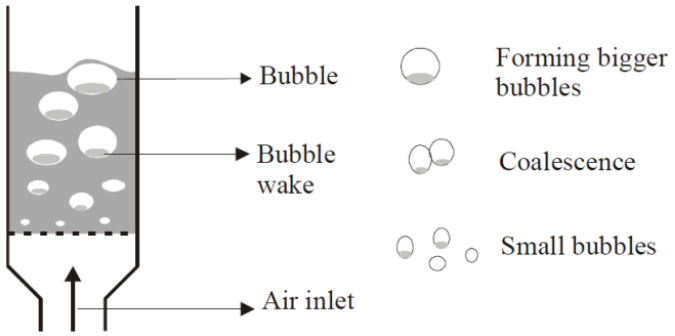

Figure 2.4 Bubbling fluidized bed and coalescence of bubbles

The pressure gradient through a fixed bed increases with increasing superficial gas velocity until minimum fluidization occurs. At minimum fluidization gas velocity is blown through the particles resulting in a pressure drop as shown in Figure 2.5.

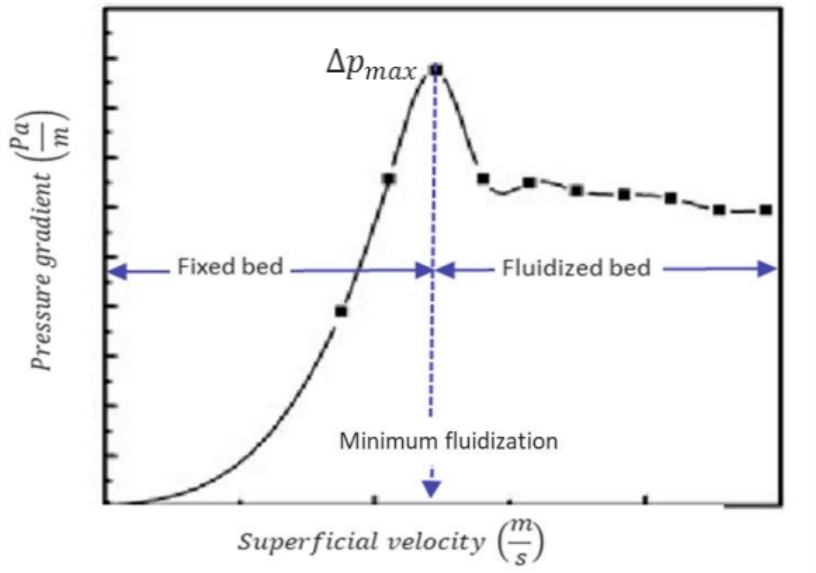

Figure 2.5 Pressure drop profile

The condition of emerging fluidization can be described by Ergun (Niven, 2002) equation which considers the pressure drop;

$$\frac{\Delta P}{L} = 150\frac{(1-\varepsilon_{mf})^2}{{\varepsilon_{mf}}^3}\frac{\mu U_{mf}}{(\emptyset_s d_p)^2} + 1.75\frac{(1-\varepsilon_{mf})}{{\varepsilon_{mf}}^3}\frac{\rho_g {U_{mf}}^2}{\emptyset_s d_p} \quad (2.1)$$

To use Ergun equation, the minimum fluidization voidage, ε_{mf}, must be known. Wen and Yu (Niven, 2002) developed the expression below based on experimental data:

$$\frac{1-\varepsilon_{mf}}{\emptyset^2{\varepsilon_{mf}}^3} \approx 11 \ \ and \ \ \frac{1}{\emptyset{\varepsilon_{mf}}^3} \approx 14$$

Combining Ergun's equation (2.1) with Wen and Yu expression we obtain the

$$Re_{mf} = \frac{d_p \cdot U_{mf} \cdot \rho_g}{\mu} = \sqrt{33.7^2 + 0.0408\frac{d_p^3 \cdot \rho_g \cdot (\rho_s - \rho_g) \cdot g}{\mu^2}} - 33.7 \quad (2.2)$$

Also, from experimental methods (Niven, 2002), a simplified equation is obtained which can be used when Reynolds number is below 20.

$$U_{mf} = \frac{d_p^2(\rho_s - \rho_g)g}{1650\mu} \quad (2.3)$$

2.2 Minimum bubbling velocity

The fluidizing velocity at which bubbles are first observed is called the minimum bubbling velocity, U_{mb}. In gas-solid beds of large particles, bubbles appear as soon as the gas velocity exceeds U_{mf}; hence $U_{mb} \approx U_{mf}$. U_{mb}/U_{mf} strongly depends on the weight fraction of particles smaller than 45 μm; P45μm and is given by Eq. 2.4.

$$\frac{U_{mb}}{U_{mf}} = \frac{2300{\rho_g}^{0.126}\mu^{0.523}exp(0.716P_{45\mu m})}{{d_p}^{0.8}(\rho_s - \rho_g)^{0.93}g^{0.934}} \quad (2.4)$$

From (Abrahamsen & Geldart, 1979) Eq. 2.4 has been modified to;

$$U_{mb} = 2.07exp(0.716P_{45\mu m})\frac{d_p{\rho_g}^{0.06}}{\mu^{0.347}} \quad (2.5)$$

2.3 Terminal velocity

2.3.1 Single particle

Terminal velocity is the maximum velocity attainable by an object as it falls through a fluid. Terminal velocity is obtained when:

$$Drag\ Force + Buoyancy\ Force = Gravity\ Force$$

- Buoyancy force is given by equation (2.6)
  $F_B = V_b * \rho_f * g$ (2.6)
- Gravity force is given by equation (2.7)
  $F_G = V_p * \rho_p * g$ (2.7)

- Drag force is given by equation (2.8)

$$F_D = \frac{1}{2} C_D * \rho_f * U^2 * A_P \tag{2.8}$$

Inserting equation (2.7) - (2.8) into (2.6) and solving for terminal velocity U_t:

$$U_t = \sqrt{\frac{4*g*D_p}{3*C_D}\left(\frac{\rho_p - \rho_f}{\rho_f}\right)} \tag{2.9}$$

Where, C_D is drag coefficient, D_p is particle diameter, ρ_p is particle density, ρ_f is fluid or gas density.

Figure 2.6 illustrates the forces acting on a single particle for a fixed bed and a fluidized bed.

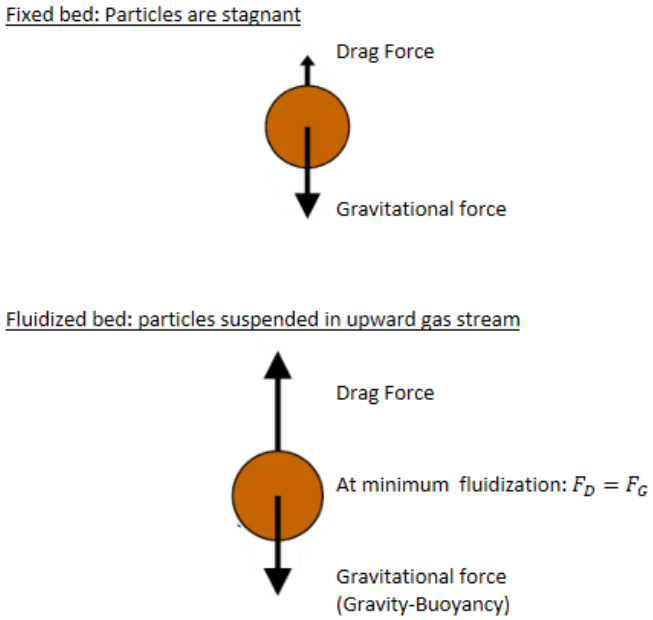

Figure 2.6 Forces acting on a single particle

2.3.2 The empirical equations for group of particles

The equation for terminal velocity based on forces acting on a single particle is not valid. Empirical equations are developed to estimate terminal velocity for groups of particles. One model is developed by (Haider & Levenspiel, 1989) to estimate for the terminal velocity of particles.

$$U_t = U_t^* \left[\frac{\mu(\rho_s - \rho_f)g}{{\rho_f}^2}\right]^{\frac{1}{3}} \tag{2.10}$$

Where;

$$U_t^* = \left[\frac{18}{(d_p^*)^2} + \frac{2.335 - 1.744\emptyset_s}{(d_p^*)^{0.5}}\right]^{-1} \quad for\ 0.5 < \emptyset_s < 1 \tag{2.11}$$

$$U_t^* = \left[\frac{18}{(d_p^*)^2} + \frac{0.59}{(d_p^*)^{0.5}}\right]^{-1} \qquad for\ \emptyset_s = 1 \tag{2.12}$$

The dimensionless particle diameter d_p^* can be calculated from equation (2.13);

$$d_p^* = d_p \left[\frac{\rho_f(\rho_s - \rho_f)g}{\mu^2}\right]^{\frac{1}{3}} \tag{2.13}$$

2.4 Binary mixture

Gas-solid flow is used in a variety of industrial processes; however, such processes are still highly dependent on empirical correlations. The minimum pickup velocity (v_{pu}) and the minimum conveying velocity (v_{mcv}) are the two most important velocities in pneumatic conveying. v_{pu} is associated with a particle that is initially at rest because it is the minimum air velocity required to initiate motion in a particle. v_{mcv} is the critical velocity below which particles will settle at the pipe's bottom. Understanding v_{pu} is essential in pneumatic conveying operations to minimize energy consumption while avoiding pipe clogging due to particle deposition and to prevent erosion and particle fragmentation (Anantharaman et al., 2016).

Due to differences in the physical properties of the two particles, such as particle size, density, and shape, the pneumatic conveying of a binary mixture can be difficult. The conveying system must be designed to transport both particles evenly and not separate throughout the process.

The minimum pickup velocity of binary mixtures of Geldart group B particles has been examined in terms of particle diameter (d_p), density (ρ), and sphericity ($\emptyset_s$) (Anantharaman et al., 2016) for pneumatic conveying systems. The key findings were that (1) d_p has a greater impact on the minimum pickup velocity than ρ and (2) particle sphericity ($\emptyset_s$) has a stronger influence on the minimum pickup velocity. Normally the minimum pickup velocity is 20% higher than the minimum conveying velocity (PowderProcess, n.d.).

Theoretical equations that can predict the fluidization behavior of homogenous beds have been developed but not for binary mixtures. The minimum fluidization velocity of a binary mixture with particles of different sizes might range from the smallest (flotsam) to the largest particle (jetsam). If the particles have different densities, the difference in minimum fluidization velocity will be more significant.

Therefore, this report is going to discover the fluidization behavior of binary mixtures with different mass ratios of filter dust and basement dust. The results will be used in pressure drop calculations. Because binary mixtures have different particle characteristics, an appropriate averaging technique is needed to define the mixture characteristics. The arithmetic mean was adopted to determine the characteristic properties as below.

$$d_{p,mix} = x_1 d_{p1} + x_2 d_{p2} \tag{2.14}$$

$$\rho_{mix} = x_1 \rho_1 + x_2 \rho_2 \tag{2.15}$$

$$\emptyset_{s,mix} = x_1 \emptyset_{s1} + x_2 \emptyset_{s2} \tag{2.16}$$

2.5 Pneumatic conveying

Pneumatic conveying is the transportation of solid particles using a moving carrier gas (typically air). For example, from a bulk transport truck to a storage silo, then to a process, then to solids/gas separation equipment. These conveying systems just require a driving force for the gas, a mechanism for delivering the product into the pipeline, and a receiving system equipped with a device to separate the product from the conveying air. Cyclones and bag filters are common separation devices used in pneumatic conveying systems. The drag force produced by the slippage between the particles and the gas overcomes frictional losses and gravitational force, giving the energy required to carry the particles from a source to a destination. When the gas velocity surpasses the terminal velocity of a particle, the particle becomes entrained in the gas flow; however, for bulk materials, that velocity tends to be somewhat greater than the terminal velocity because particles can cluster together.

Figure 2.7 depicts a variety of flow patterns that can be observed depending on the gas velocity and material properties. With a constant solids feed rate, as the gas velocity increases, the packed bed will degenerate into dunes or unstable dunes, and finally, the particles will entirely entrain into the gas stream, resulting in a homogenous flow. Particles travel faster in homogenous flow, but the solids concentration is significantly lower. Increasing the solids content while maintaining the same gas velocity has the opposite result. The hydrodynamics go from homogeneous flow to dune flow, then slug flow, and eventually plug as a packed bed.

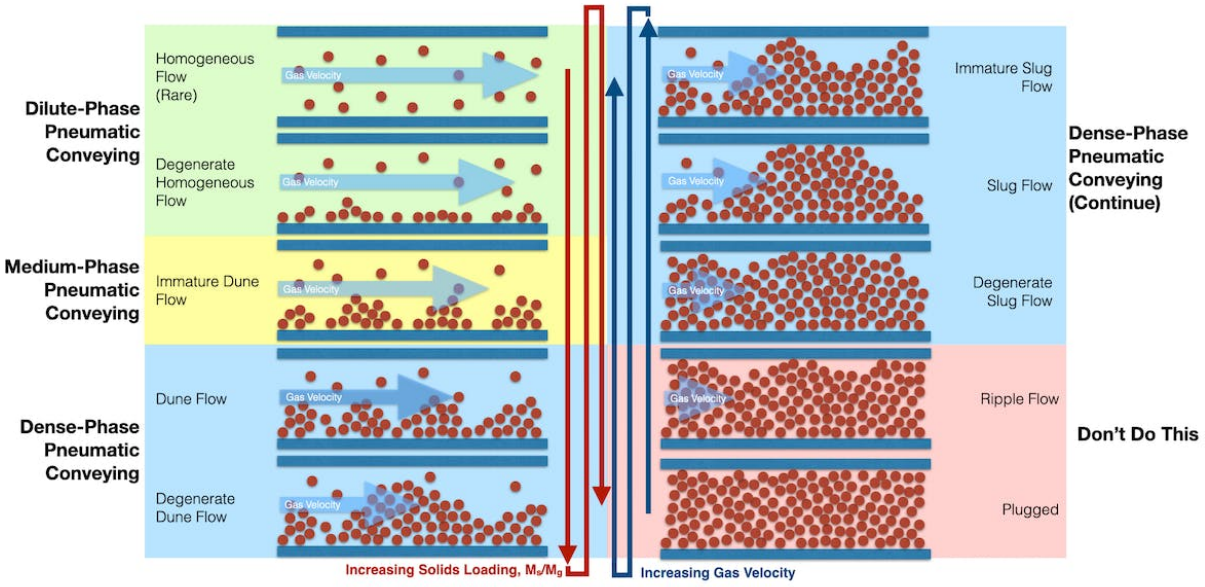

Figure 2.7 Hydrodynamic differences between dilute and dense phases (Dhodapkar & Cocco, 2022)

Homogeneous flow is easy to handle, but dune flow and slug flow are more difficult yet may be required for some applications. Higher gas velocity, lower solids concentration conveying is referred to as dense phase, whereas lower gas velocity, greater solids concentration conveying is referred to as dilute phase. To avoid unstable flow conditions, conveying occurs between these two regimes and requires careful control of gas velocity at the material pickup point.

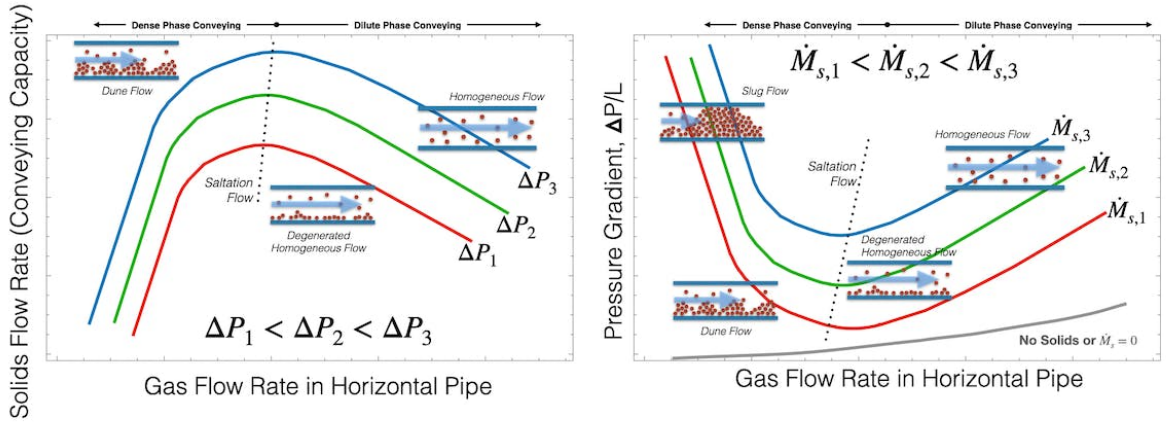

Figure 2.8 Gas flow rate versus solids flow rate (right) or pressure gradient (left) (Dhodapkar & Cocco, 2022)

2.5.1 Major components in a typical pneumatic conveying system

A pneumatic conveying system contains several components that should work together to produce the desired operating condition. Every pneumatic conveying system is typically made up of four basic components:

- **Conveying media:** As the prime mover, several types of compressors, fans, blowers, and vacuum pumps are used to convey the gas.
- **Feeding mechanism:** A feeding device, such as a rotary valve or a screw feeder, is used to feed the solid into the conveying line.
- **Conveying line:** This includes all straight pipelines with horizontal and/or vertical parts, bends, and auxiliary components like valves, diverters, etc.
- **Separation device:** The solid must be separated from the gas stream in which it was conveyed at the end of the conveying line. For these cyclones, bag filters, and electrostatic precipitators are commonly used.

2.5.2 Types of conveying systems

2.5.2.1 Simple positive pressure systems

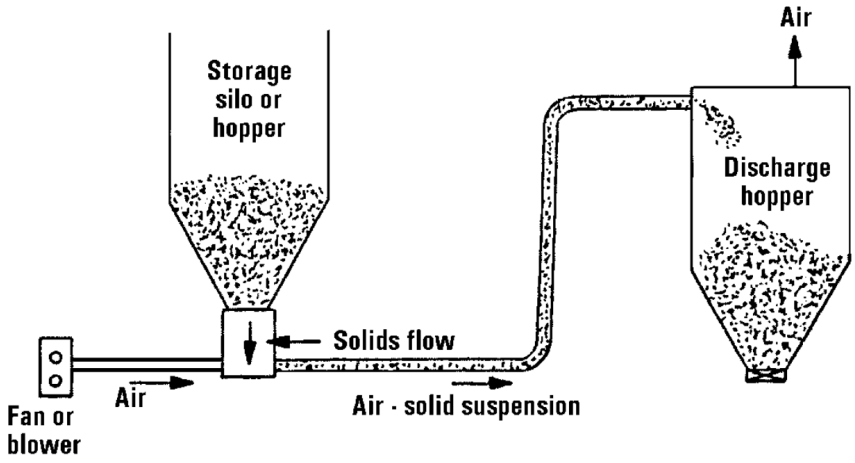

Figure 2.9 Simple positive pressure conveying system (de Silva, n.d.)

These systems typically use fans or blowers with a maximum pressure of less than one bar. Technically, the air is supplied into the pipeline via the fan or blower. Then receives material from the bottom of a storage hopper or silo. The material is subsequently carried through the pipeline in suspension with the air to the discharge point. This is generally another hopper or silo from which the material is gravity discharged. A typical plant layout is shown in Figure 2.9.

2.5.2.2 Complex Positive Pressure Systems

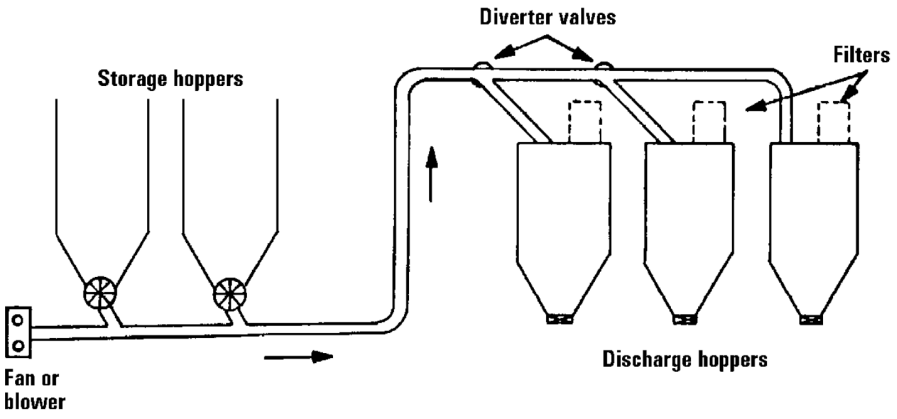

Figure 2.10 Complex positive pressure system (de Silva, n.d.)

Diverter valves allow for multiple deliveries from various sources to various receiving locations, allowing for the development of extremely versatile systems. Figure 2.10 depicts an example of a typical plant layout.

2.5.2.3 Simple Negative Pressure Systems

Figure 2.11 depicts an example of a simple negative pressure conveying system. Feeding into a negative pressure system is simpler than feeding into a positive pressure system, although care must be given not to choke the inlet. These systems are frequently used to transport resources from several sources to a single point. Vacuum systems have the distinct benefit that all gas leakage is inward, resulting in almost negligible dust emission into the environment. This is especially important for toxic or explosive substances.

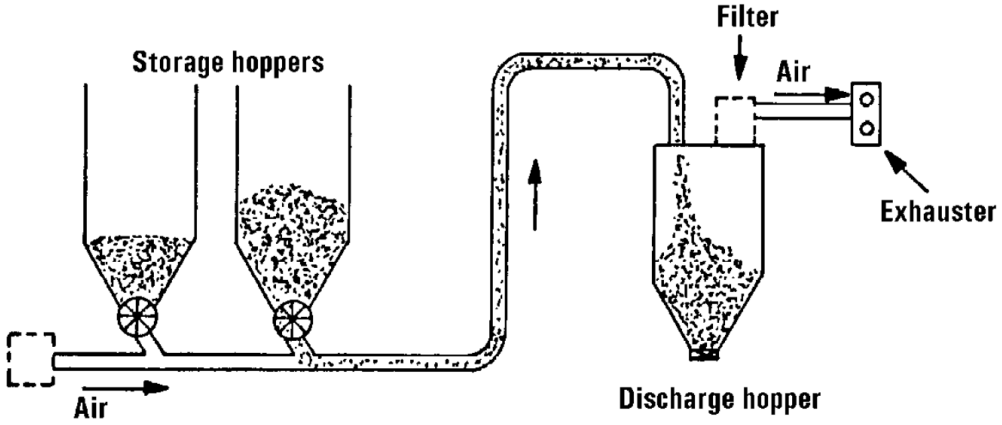

Figure 2.11 Simple negative pressure system (de Silva, n.d.)

2.5.2.4 Combined Negative and Positive Pressure Systems

It is not recommended to transport the product through the fan due to deterioration and erosion issues. This can be avoided by using an intermediate storage hopper with its own filter and feed system, as illustrated in Figure 2.12. They are one of the most adaptable kinds of pneumatic conveyors, capable of transporting material from various sources to many discharge points. They are also known as "pull-push" or "suck-blow" systems.

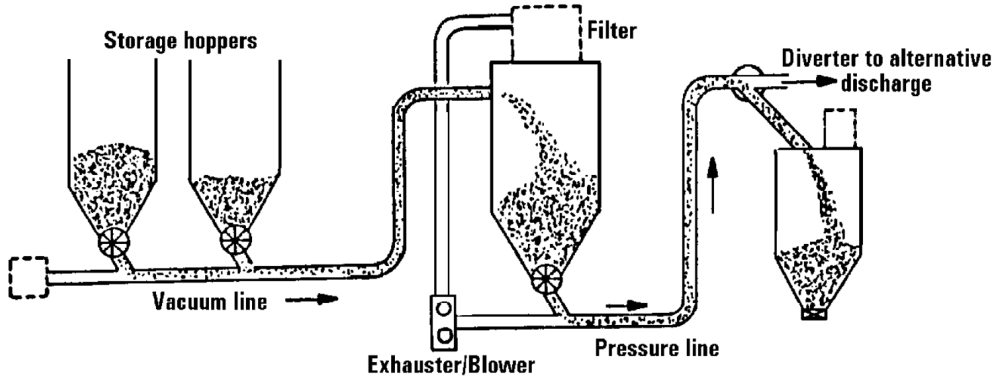

Figure 2.12 Combined negative and positive pressure system (de Silva, n.d.)

2.5.3 Modes of Pneumatic Conveying

Pneumatic conveying systems can be classified into several modes for the convenience of use. Based on the particle concentration in the pipeline, pneumatic conveying systems are divided into two categories (de Silva, n.d.).

- Dilute phase
- Dense phase

For simplicity, each phase is classified based on the mass loading ratio as shown in Table 2.1. Mass loading ratio (μ) is defined as the mass flow rate of solids conveyed divided by the mass flow rate of air utilized.

Table 2.1 Classification based on mass loading ratio

Mode	$\boldsymbol{\mu}$
Dilute phase	0-15
Dense phase	>15

2.5.4 Design of a pneumatic conveying system

According to Figure 2.8 the carrying capacity vs. gas flow rate, the carrying capacity at a given system pressure drop reaches a maximum as the gas flow rate increases. The maximum increases as the pressure drop across the system increases. This maximum is often the transition point between dense and dilute phase conveying. This may appear to be an ideal operating condition, but it is not. The flow hydrodynamics at maximum carrying capacity corresponds to the saltation flow, which is the point at which particles drop (or salt) out of the flow stream as the gas velocity declines. Flow is unsteady at this point, therefore operating at or near this point in a commercial system is difficult. Dilute phase systems are intended to operate at gas speeds somewhat higher than the saltation velocity. Below this limit, dense phase systems function.

For single-phase gas flow, the pressure gradient vs gas flow rate curve (in Figure 2.8) approximates a monotonic, velocity-squared trend. Nevertheless, when solids are added to the horizontal conveying line, the pressure gradient changes dramatically. This is due to the presence of solids causing additional pressure drop components such as particle acceleration, particle shear stresses, and particle-wall friction, all of which are more important than the corresponding gas acceleration, gas shear stress, and gas-wall friction.

It is advisable to operate near, but not on, the saltation flow line where the pressure gradient is the lowest, implying that less capital and power are needed. Moreover, with dense phase flow to the left of the saltation flow line, a low gas flow might result in a packed bed that blocks the line and does not move. The pressure gradient and pressure fluctuations are greater in dense phase mode than in dilute phase mode, resulting in vibration in the conveying line. The pressure changes less in dilute phase flow, which occurs at high gas velocities and to the right of the saltation flow line, causing fewer concerns about mechanical stress from vibration.

2.5.5 Pressure drop calculation

In pneumatic powder conveying systems, the system's performance is impacted by the pressure drop, making it an essential parameter to consider. The pressure drop is the difference in pressure between the inlet and outlet of the conveying pipeline. The theory and calculation procedures for developing a dilute phase pneumatic conveying system are described in this section. It is based on the research of (Zenz & Othmer, 1960). While various additional methods

have subsequently been developed, this method has been widely employed and has been proven to be within 10% of the observed pressure drop.

Design calculations for a dilute phase conveying system are based on estimating the pressure drop in the system caused by the movement of gas and particles. According to (Zenz & Othmer, 1960), this pressure decrease is constituted of six effective forces for both dilute and dense phase conveying:

1. Friction of the gas against the pipe wall
2. Force required for moving the solids mass through the conveying pipeline
3. In vertical pipes the force required to support the weight of the solids
4. In vertical pipes the force required to support the weight of the gas
5. Force required to accelerate the solids
6. Friction between the pipe and the solids

Compared with the dense phase, friction between the pipe and the solids can be neglected in dilute phase conveying.

The next step is to have a single equation for determining the total pressure drop in a conveying system with both horizontal and vertical lines. Also, the term ΔP_{misc} was introduced to account for pressure drop in any equipment necessary at the end of the conveying line, such as a dust collector.

$$\Delta P_T = \Delta P_{acc} + \Delta P_a + \Delta P_s + \Delta H_a + \Delta H_s + \Delta P_{misc} \tag{2.17}$$

For horizontal pipes

For horizontal lines, the pressure drop is caused by gas acceleration, solid acceleration, friction between the gas and the pipe wall, and solid flow through the pipeline. An additional term (WL/V_p) is added to indicate the weight of the supported solids in a vertical line for vertical flows.

For vertical lines:

$$\Delta P_{T,VERT} = \Delta P_{T,HOZ} + \frac{WL}{V_p} \tag{2.18}$$

Gas-only pressure drop

Pressure drop of gas is due to frictional losses between gas and the conveying pipeline and in any bends, diverter valves, and flexible hoses that may be in the pipeline. (Wypych & Arnold, 1987) has presented an empirical correlation as in Eq. 2.15 to calculate gas only pressure drop.

$$\Delta P_g = 0.5\left[(101^2 + 0.004567\dot{m}_a{}^{1.85} L D^{-5})^{0.5} - 101\right] \tag{2.19}$$

Note: In the above expression, the term "L" is the length of the straight sections of the pipeline and is the "equivalent length" of the bends, diverter valves, and flexible hoses.

Pressure drop due to acceleration

Particles must be fed into the gas stream for every pneumatic conveying system, and there is an interval during which the particles and gas are not in a steady state. Whenever there is a change of direction, such as a bend or a valve, the particles decelerate and accelerate. In a simple model, (Woodcock & Mason, 1987) this additional pressure component was calculated by the following model (Eq. 2.20).

$$\Delta P_{acc} = \frac{\dot{m}_s V_p}{A} \tag{2.20}$$

Solid flow pressure drop

(Weber, 1982) has proposed a method to determine the pressure drop due to solids particle in horizontal pipe sections,

$$\Delta P_s = \lambda_s \mu \rho_a {u_c}^2 \frac{\Delta L}{2D} \tag{2.21}$$

λ_s can be expressed as a function of Frode number based on pipe diameter; Fr_D

$$Fr_D = \frac{u}{\sqrt{gD}} \tag{2.22}$$

Some developed correlations to describe the additional pressure drop factor are reported by (Naveh et al., 2017) and the formula in Eq. 2.23 will be used in this study.

$$\lambda_s = 0.005 \frac{1 - {Fr_D}^{-1}}{1 + 0.00125 {Fr_{fo}}^{*2}} \tag{2.23}$$

And Frode number based on free fall velocity (terminal settling velocity) is defined as;

$${Fr_{fo}}^* = \frac{w_{fo}}{\sqrt{g * D}} \tag{2.24}$$

Pressure drop due to elevation of gas by ΔZ

$$\Delta H_a = \Delta Z \rho_g \tag{2.25}$$

Pressure drop due to elevation of solids by ΔZ

$$\Delta H_s = \frac{\Delta Z W g}{V_p} \tag{2.26}$$

Pressure drop due to miscellaneous equipment in the conveying system

This term is a constant. Assume that it is in a dust collector at the end of the conveying line and is 0.2 psi/1378,95 Pa (Agarwal, 2005).

Minimum conveying/saltation velocity

The transport air velocity is a critical parameter. Inadequate air velocity causes pipeline blockage, whereas excessive air velocity causes pipe erosion and product deterioration. In general, minimum-conveying velocity is defined as the lowest safe gas velocity for horizontal

solid transport. If this gas velocity is set at the feed point, the gas velocity will increase down the pipeline due to compressibility effects, i.e., density drop, and the remainder of the pipeline should operate well over this lower velocity limit.

For particles of diameter < 1 mm:

$$v_{mcv} = \frac{0.25\sqrt{Dg}}{\sqrt{\frac{\rho g}{\rho s}}} \tag{2.27}$$

Choking velocity in vertical flows

Choking velocity is the minimum velocity necessary to maintain a continuous flow without blockage or "choking" in vertical pneumatic conveying systems. The choking velocity is defined as the point in the pipeline when the pressure drop equals the weight of the material per unit area, causing particles to accumulate resulting in a pipe blockage. It can be estimated using the following equation (Yang, 1975):

$$\frac{2gD(\varepsilon_c{}^{-4.7}-1)}{[U_c-U_t]^2} = 6.81 \times 10^5 \left(\frac{\rho_a}{\rho_s}\right)^{2.2} \tag{2.28}$$

To ensure a smooth and uninterrupted flow without blockages or plugging, the choking velocity is an important parameter that must be addressed throughout the design and operation. If the conveying velocity is less than the choking velocity, the material can accumulate and block the pipeline, resulting in system failure, decreased efficiency, and costly downtime.

Solids velocity (V_p)

Because of the drag forces between the gas and the solids, solid velocity is always smaller than gas velocity. This difference is referred to as the slip factor. This slip factor is around 0.8 for most coarse or hard materials, implying that the solid velocity is 80% of the gas velocity. i.e.,

$$V_p = 0.8 * V_a \tag{2.29}$$

Solids velocity in long radius bends

At a 90-degree radius bend, the velocity at the bend exit V_{p2} is 0.8 times the velocity at the bend entrance V_{p1}. The factor "0.8" is a common number, however, it can range between 0.6 and 0.9 depending on the solid characteristics. The exit velocity V_{p2} for bends less than 90^0 is given by Eq. 2.28.

$$V_{p2} = \left[1 - \frac{degree\ of\ bend}{90}(1 - 0.8)\right] V_{p1} \tag{2.30}$$

Gas Density along the Conveying Line

Gas density is affected by gas pressure and temperature. Gas temperature is considered to remain constant in most conveying systems as it is an isothermal expansion. As a result, only the changes in pressure will cause variations in gas density. When pressure increases or decreases along the conveying line, depending on whether it is a vacuum or pressure system, gas density will simultaneously increase or decrease.

Gas Density, Gas Pressure, and Gas Velocity Calculations

Outlet gas density is calculated by using the formula = (28·Outlet Pressure)/ (8.314· (Outlet Temp. + 273.15))

Outlet gas velocity is calculated by using the formula: = Inlet gas velocity X (Inlet gas density/outlet gas density).

Note: Mass flow rates remain constant. Since the densities are changing volume flow rates change accordingly.

Pipe Equivalent Length (L)

- For straight pipes use the actual length of the pipe.
- For components such as bends, diverter valves, and flexible hoses, use their equivalent length expressed in pipe diameters of the conveying pipe. Typical equivalent length values are given in Table 2.2.

Table 2.2 Pipe Equivalent Lengths (Agarwal, 2005)

Component	Equivalent Length
Bends: 90^0 bend, long radius (10 to 1 radius to diameter ratio)	40, or 20 ft (12.192 m, or 6.096 m)
Diverter valves: 45^0 divert angle 30^0 divert angle	 20 ft (6.096 m) 10 ft (3.048 m)
Flexible Hoses: Stainless steel, with lined interior Rubber or vinyl hose	 3 x pipe length 5 x pipe length
For bends that are less than 90°, use the equivalent length as 40×Degree of Bend/90^0	

3 Survey of dusting in an Aluminium plant

3.1 Situation at the crushing and storage area

At one of Hydro's aluminium plants dusting in the crushing and storage area of the anode cover material plant has been an environmental issue that requires further work and retrofit of existing bulk solids handling equipment and logistics. The source of dusting has been identified as coming from uncontrolled mixing of two material flows: filter and potroom basement dust. The two materials are two of the ingredients of ACM for potrooms. ACM quality has not been a key performance indicator (KPI) for the aluminium plants, focus is on quantity, that is, to have enough ACM material in the main silos to cover the anodes.

Figure 3.1 Hydro's storage area of ACM plant

The first step of sampling filter dust was to find a suitable sampling point by opening an existing flange and sampling in a bucket. The method was not satisfactory, it was just an attempt to sample some dust for the chemical analysis, filter dust containing approximately 53.4 % reacted Alumina, 41.3 % Fluorides and 4% Carbon. Basement dust has a similar chemical composition.

Potroom basement dust was collected directly from the floor (Figure 3.2). The next step was to establish a temporary sampling point and for two weeks operate the plant without filter and basement dust. Around 50 tones of filter dust were collected in big bags marked as FS (Figure 3.4) and stored on site. Filter dust used for the experiments in this work comes from random sampling from the big bags. Environmental measurements of dust before and after removing the dust from the crushing plant showed a reduction in dust levels, thus a potential to improve the working area at the anode crushing and storage plant.

Figure 3.2 Basement dust colleting from the floor

Figure 3.3 Dust samples

Figure 3.4 Sampling of filter dust

4 Theoretical calculations

This chapter contains calculations of the minimum fluidization velocity, bubbling velocity, and terminal settling velocity of particles and a comparison of dust particles with Secondary Alumina. Table 3.1 shows the physical properties that have been used for theoretical calculation and they were measured at SINTEF powder hall.

Table 4.1 Physical properties

	density [kg/m^3]	Bulk density (loosely packed) [kg/m^3]	Viscosity [Pa.s]	d_p mean [µm]	Sphericity	Fines content wt.%	Void fraction (loose packed)
Air	1.2	-	1.8348E-05	-	-	-	-
Secondary Alumina	3777	985	-	99.02	0.84	0.14	0.74
Filter dust	3489	1146	-	75.48	0.65	0.35	0.67
Basement dust	3511	1115	-	83.80	0.83	0.30	0.68

4.1 Mean particle diameter

The particle size distributions for dust samples are shown in Figures 3.1 to 3.3. The average particle size are 99.02 µm, 75.48 µm, 83.80 µm respectively for secondary Alumina, filter dust, and basement dust.

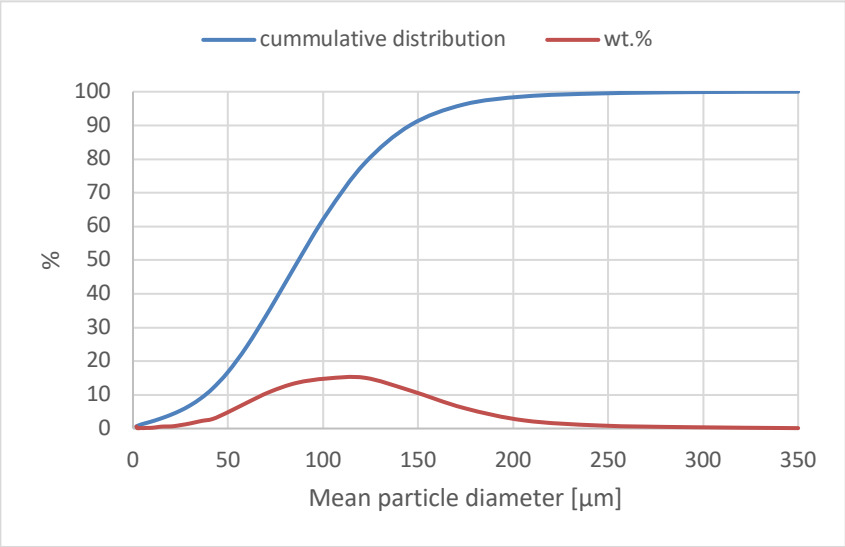

Figure 4.1 Particle size distribution of secondary Alumina

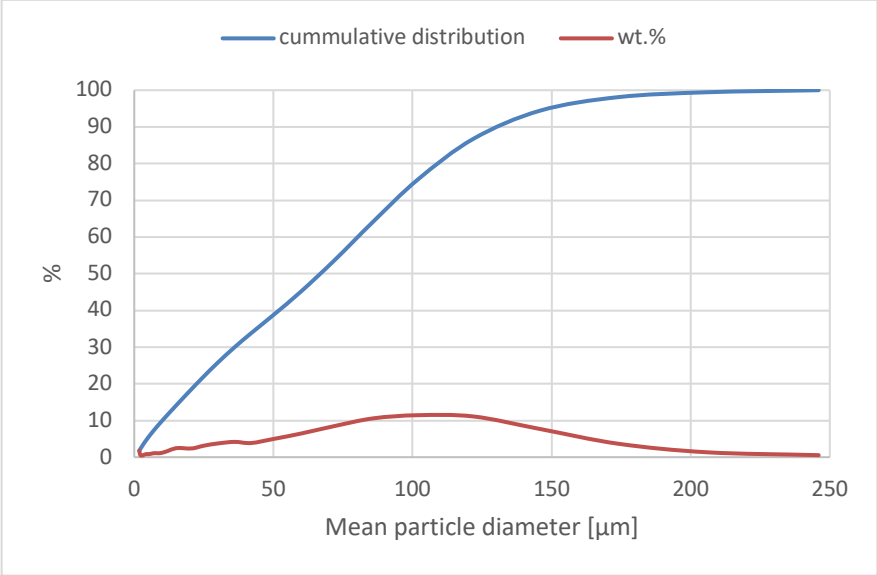

Figure 4.2 Particle size distribution of filter dust

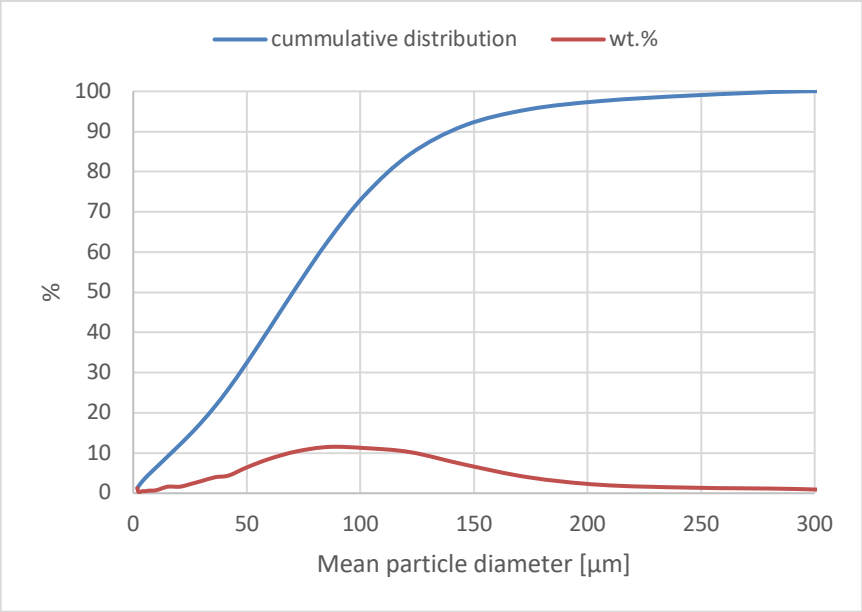

Figure 4.3 Particle size distribution of basement dust

4.2 Minimum fluidization velocity

For calculating the minimum fluidization velocity, equation 2.3 is used. Weighted average U_{mf} is calculated considering the whole particle size distribution for the dust samples and compared with secondary Alumina which is shown in Appendix A. Figure 3.4 to 3.6 illustrate the variation of minimum fluidization velocity with particle diameter. The average minimum fluidization velocities for secondary Alumina, filter dust, and basement dust are 1.487 cm/s, 0.934 cm/s, and 1.145 cm/s respectively.

4.3 Minimum bubbling velocity

Eq. 2.5 was used for minimum bubbling velocity calculations for dust particles. Appendix B shows the U_{mb} values calculated for the PSD of each dust type. From Figures 3.4 to 3.6 it is evident that both the minimum fluidization velocity and minimum bubbling velocity increase with increasing particle diameter. The values are 1,008 cm/s, 0,893 cm/s, and 0,957 cm/s respectively

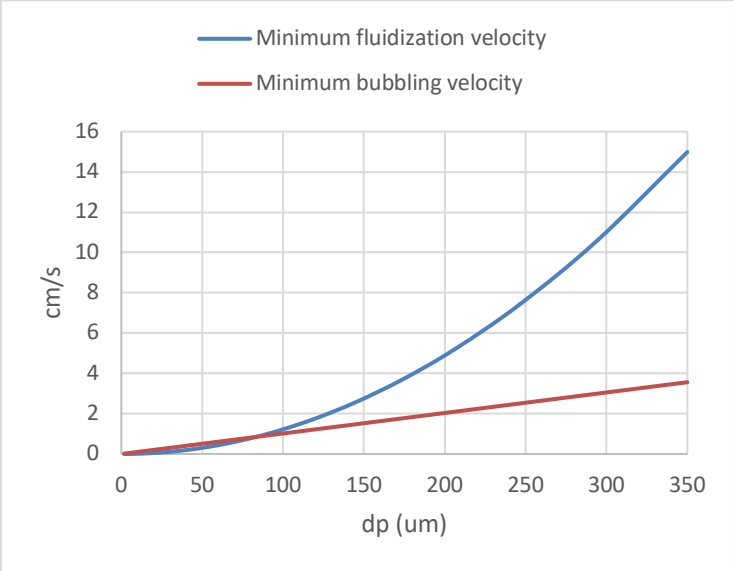

Figure 4.4 Minimum fluidization velocity and minimum bubbling velocity of secondary Alumina

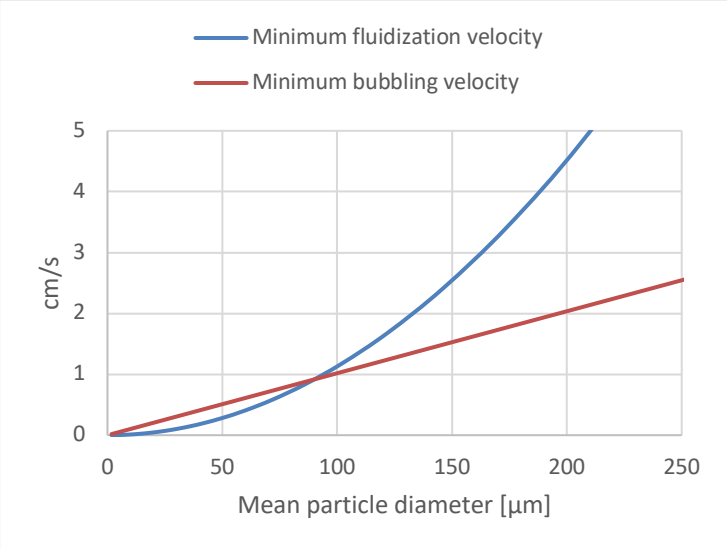

Figure 4.5 Minimum fluidization velocity and minimum bubbling velocity of filter dust

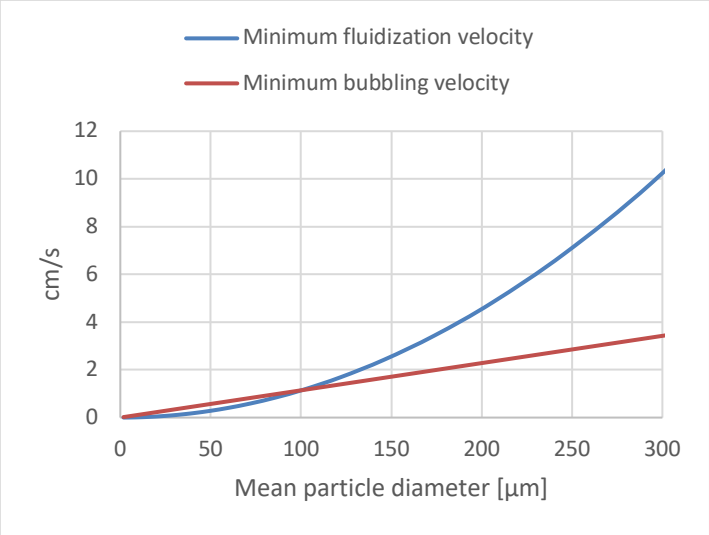

Figure 4.6 Minimum fluidization velocity and minimum bubbling velocity of basement dust

4.4 Terminal settling velocity

For calculating terminal settling velocity, Haider and Levenspiel method is used (Eq. 2.9). Haider and Levenspiel method is used for whole particle size distribution and the weighted average was calculated as shown in Appendix B. Figure 3.7 to 3.9 show terminal settling velocities for all particles.

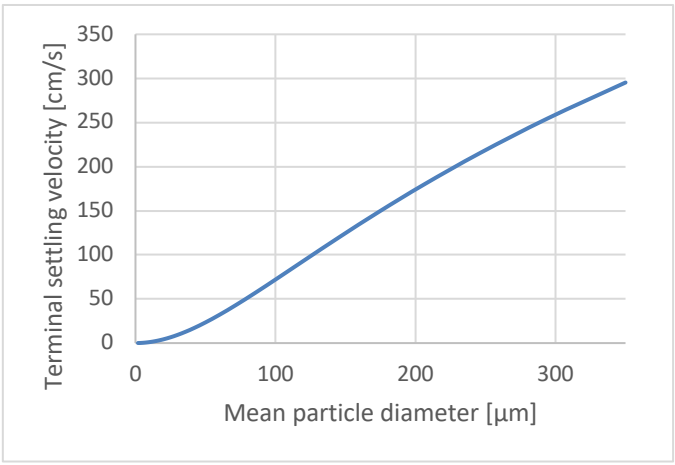

Figure 4.7 Terminal settling velocity of secondary Alumina

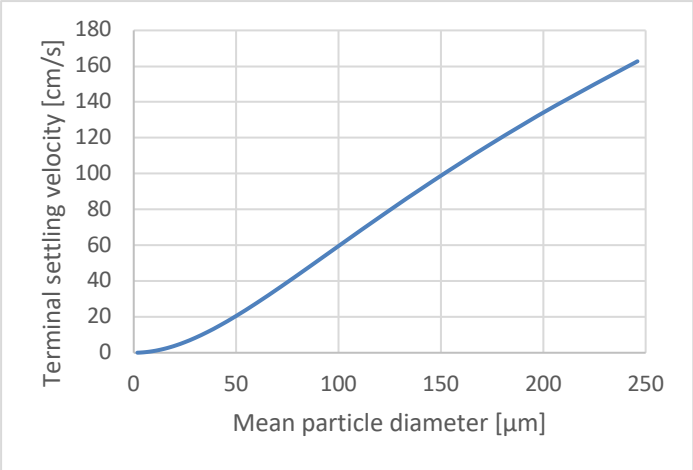

Figure 4.8 Terminal settling velocity of filter dust

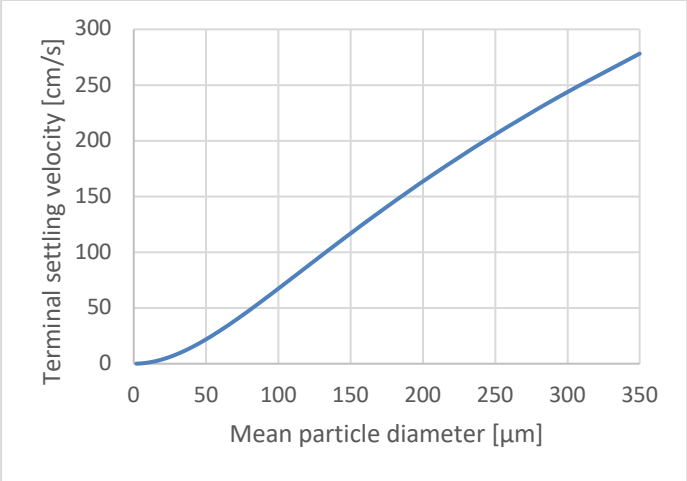

Figure 4.9 Terminal settling velocity of basement dust

4.5 Comparison of dust particles

Figures 3.10 and 3.11 show a comparison between dust particles and secondary Alumina. With increasing particle size theoretical U_{mf}, U_{mb}, and U_t are increasing. Table 3.2 shows the results of the calculations.

Table 4.2 Theoretical calculation results

	Secondary Alumina	Filter dust	Basement dust
d_p mean (um)	99,02	75,48	83,80
U_{mf} mean (cm/s)	1,487	0,934	1,145
U_{mb} mean (cm/s)	1,008	0,893	0,957
U_t mean (cm/s)	72,778	42,813	55,421

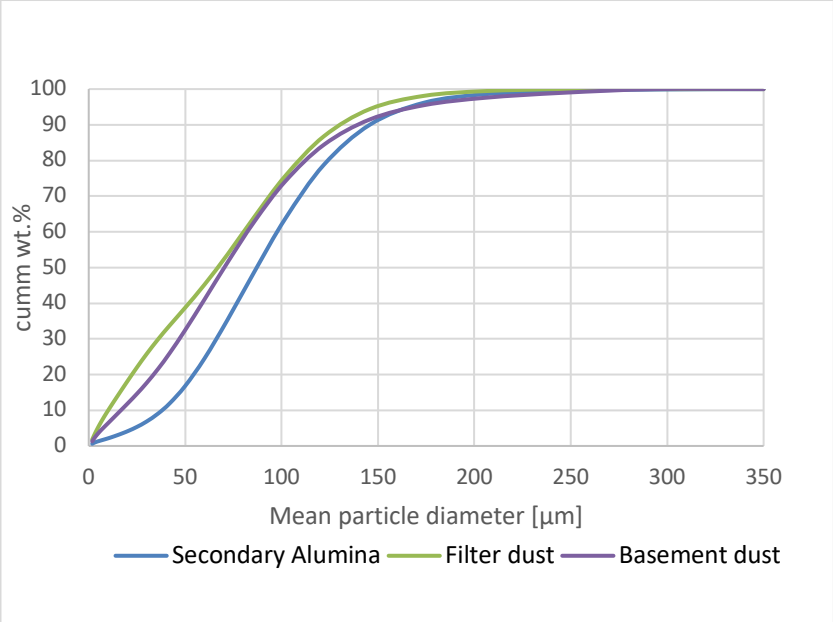

Figure 4.10 PSD of dust particles

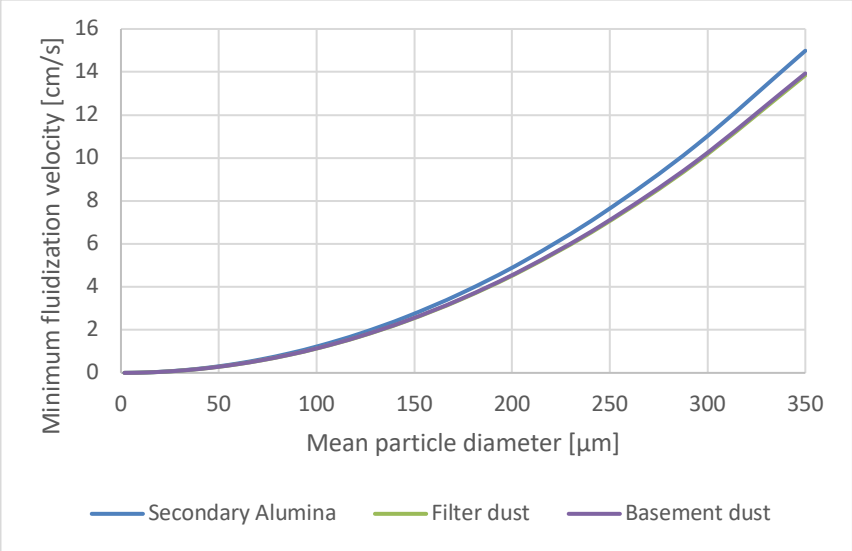

Figure 4.11 Comparison of U_{mf}

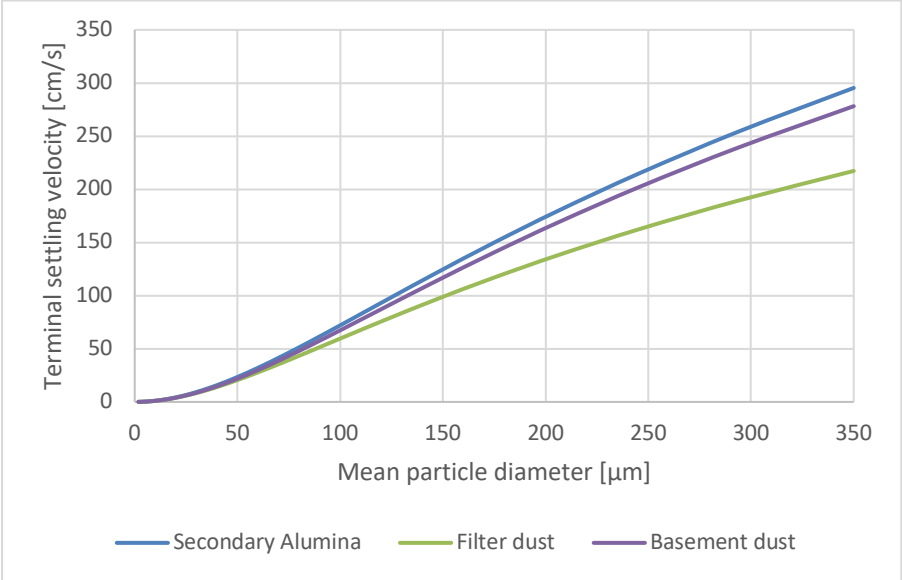

Figure 4.12 Comparison of U_t

Table 3.2 shows how U_{mf}, U_{mb}, and U_t increase with increasing particle sizes. And these dust particles lie at the margin of Geldart A and B groups. Normally, for Geldart Group B (particle diameter, dp ~ 100–800 µm), $U_{mf} \approx U_{mb}$, as a result, there is no range of gas velocities across which particles may mix without generating gas bubbles. As compared to fixed beds, bubbles in fluidized beds can reduce gas-solid interaction. For Geldart A particles (dp ~ 20–100 µm) $U_{mf} < U_{mb}$. However, note that in this study $U_{mb} < U_{mf}$ which is opposite to existing studies. There is no clear explanation for this scenario, but it can happen due to the models used in calculations.

5 Experimental methods

The following chapter contains the experimental setup, procedure for fluidization experiments, and particle characterization tests held at the powder hall.

5.1 Experimental set-up

5.1.1 Fluidized bed

Experiments were carried out in the laboratory on a fluidized bed constructed of Lexan plastic in a cylindrical shape. The tube is made up of an air distributor that is coupled to an air supply at the bottom. Nine pressure transmitters are mounted throughout the tube, and the pressure data are recorded using a LabVIEW® program. The tube's height from the air distributor is 1.4 m, and its diameter is 0.084 m. Figure 4.1 depicts the rig's design and laboratory setup.

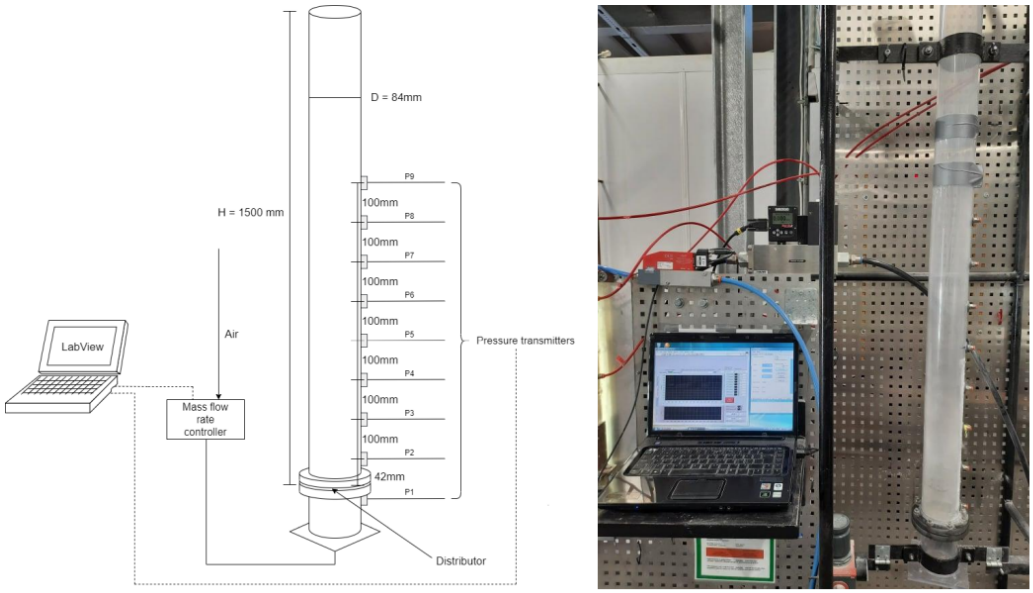

Figure 5.1 Schematic of the experimental rig set up (left) and laboratory setup (right) (Aavik et al., 2021)

5.1.2 Air flow meter

To measure the air flow rate within the required superficial air velocities three different types of flow meters were used. Mass flow meter-1 was used to measure air flow rates of 0-4 NLPM. Mass flow meter-2 was for flow rates between 4-120 NLPM and then over 120 NLPM flow meter-3 was used.

Table 5.1 Mass flow meters

	Mass flow meter-1	Mass flow meter-2	Mass flow meter-3
Model	SIERRA 8225-M-3-0V1-PV1-V1-MP	Wöatlin GSC-D4SA-BB12	SIERRA C100H2-DD-17-0V1-SV1-PV2-V1-54-C3-CC
GAS	Air	Air	Air
Output Signal	0-5 VDC	4-20 mA	0-5 VDC/ 4-20 mA
Connections	3/8" COMP	-	DN20FLANGE
Orientation	Horizontal	Horizontal	Horizontal
Inlet Pressure	4 bar g	6 bar a	4.5 bar g
Outlet pressure	-	1.1 bar a	0.5 bar g
Operating Temp	20°C	-	20°C
Maximum Temp	50°C	-	50°C
Range & Units	0-94.8 NLPM	200 NLPM	0-1000 NLPM
Supply	12-15 VDC	-	24 VDS
Maximum Pressure	500 psi g.	-	500 psi g.
STP	0°C	0°C/1013.25 mbar a	21°C/760 mm Hg

5.2 Experimental procedure

This section outlines all the laboratory tests and experiments performed on dust samples, particle size distributions, sphericity, particle and bulk densities, and fluidization experiments for both pure dust samples and binary mixtures.

The experimental rig and surrounding equipment were cleaned before conducting the experiments to avoid contamination. Pressure sensors and air supply tubes were connected, and the joints were inspected for leakage. The required particle weight was measured using an electronic scale and carefully fed into the FB rig from the top end. The material should be enough to cover both the P2 and P3 pressure sensors. The bed height was measured in each case. The pressure drop (P2-P3) vs. gas superficial velocity graph was obtained by increasing the air velocity from zero. This graph can be used to determine the minimum fluidization velocity.

Pressure variations over time graphs revealed that the system reached a pseudo-steady state after about 160-200 s. Therefore, after 200 seconds of each superficial velocity value, pressure drop data were obtained, and the velocity was continuously increased. Table 5.2 shows two kinds of experiments planned: pure particles and binary mixtures. A suction device was placed on top of the rig to collect entraining particles. In each case, pressure drop profiles were obtained using the Python program used for data extraction (Appendix E). The gas velocities (Nm/s) were calculated by dividing the airflow rates (NLPM) by cross-sectional area of the FB rig (m^2). Pressure drop is denoted by ΔP23 (mbar) and is the difference between PT2 and PT3 pressure measurements.

5.2.1 Pure particle experiments

Three types of particles were used for pure particle experiments. (1) Secondary Alumina (2) Filter dust, and (3) Basement dust. Fluidized bed experiments were conducted with Secondary Alumina to compare the results with dust particles. First, PSD and other particle characteristics; i.e., particle and bulk densities, sphericity, and fines content were measured at SINTEF powder hall which are used in theoretical calculations. After cleaning the rig, a sample of 2 kg was weighed and poured into the column in each case and supplied compressed air. The operating air velocity was increased from 0 to 1.26 m/s (0-400 NLPM) to obtain experimental U_{mf}, U_{mb}, and U_t to validate theoretical calculations.

5.2.2 Binary mixture experiments

The initial plan was to premix different mass ratios of filter dust and basement dust as shown in Table 4.2 and conduct the fluidized bed experiments to observe the fluidizing behavior and to obtain terminal settling velocities for pressure drop calculations. Unfortunately, during experiments the rig was damaged and had only a limited time. Therefore, U_{mf} and U_t were determined theoretically and used in pressure drop calculations as described in section 2.4.

Table 5.2 Binary mixture ratios

Mixture	Filter dust wt.%	Basement dust wt.%
M1	80	20
M2	70	30
M3	60	40

5.3 Pipeline configuration

The pipeline configuration “A” at the Powder Hall was used in pressure drop calculations. A schematic diagram of the pipeline configuration (“A”) is shown in Figure 4.2.

Let's assume a pressure-type dilute phase pneumatic conveying system conveying binary mixtures of filter dust and basement dust at different ratios at three different mass flow rates through a proposed conveying line. The pipeline's diameter and length are 0.075 m and 79 m respectively. However, the dimensions can be changed if the calculated pressure drop is not feasible. Assume the conveying system uses ambient air at standard conditions. Starting from the inlet, the conveying line is 6 m horizontal, then has a 90^0 horizontal bend, then again 21 m horizontal section, then a 90^0 horizontal bend, then a 13 m horizontal section, then a 90^0 long radius bend, an 8.25 m vertical pipe section, a 90^0 long radius bend, an 11 m horizontal section, a 90 long radius bend, a 2.75 m vertical section, then a 90^0 long radius bend, a 10 m horizontal section, a 90^0 horizontal bend and finally a 7 m horizontal section. Ambient conditions are 101325 Pa and 25^0 C. Air density at these conditions is 1.2 kg/m^3. Solids velocity is 80% of gas velocity. The pipeline material is Steel. Pipeline absolute roughness is $0.045\times 10^{-3}\ m$.

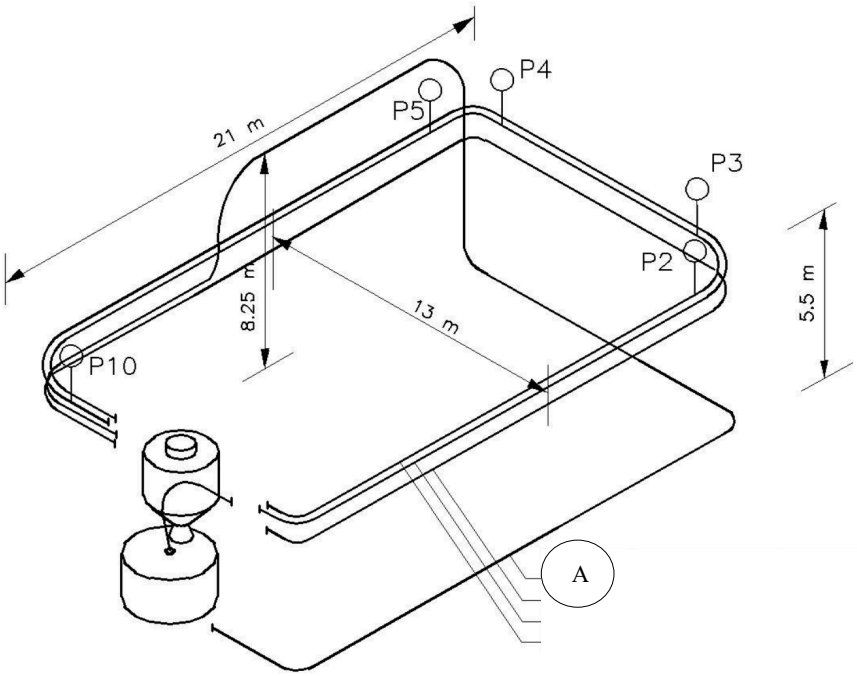

Figure 5.2 Schematic diagram of the pipeline configuration

The pressure drop is calculated piecewise, for each 2m straight pipeline section (horizontal and vertical). For bends pressure drop is calculated separately and added together to get the total pressure drop in the system. Likewise, velocities and densities were also calculated for each 2m section and after every bend. pressure drop has a great impact on system performance, thus optimizing the design to minimize pressure drop while maintaining efficient transportation is necessary.

6 Results and Discussion

6.1 Geldart classification of particles

Table 6.1 Data for Geldart classification

Material	Mean particle size (μm)	Particle density (kg/m^3)
Secondary alumina	99.02	3777
Filter dust	75.48	3489
Basement dust	83.80	3511

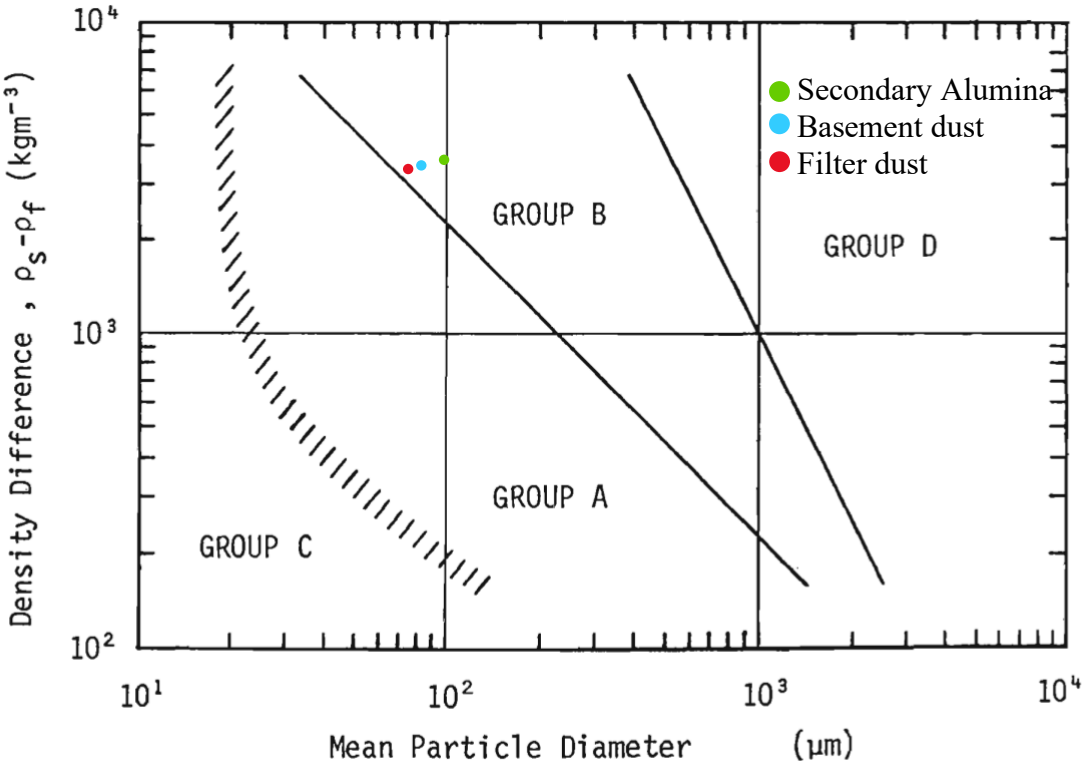

Figure 6.1 Location of materials on Geldart classification diagram

All dust samples lie within Geldart B group (at the margin of Geldart A). During fluidization also at low gas velocities particles fluidized. But due to its color and particle cohesiveness, it was hard to observe bubbling because Fb walls were covered with dust and some rat holes also appeared.

6.2 Pure particle experiments

6.2.1 Secondary Alumina

The plot (Figure 5.2) does not show the typical pressure drop profile shape. However, it shows a sudden drop when the air velocity is around 0.01 Nm/s (1.10 cm/s). This pressure drop is an indication of minimum fluidization velocity. U_{mf} should be right after this pressure drop (Norheim, 2013). The theoretically calculated U_{mf} for secondary Alumina is 1.487 cm/s. At 100 LPM (31.51 cm/s) smaller particles have already started to entrain, but most of them come back to the column. The experimental U_t can be taken as 63.04 cm/s (200 NLPM) which is close to the theoretical U_t of 72.778 cm/s.

The minimum fluidization velocity for Secondary Alumina has been estimated as 1 cm/s by Hydro Aluminium (Norheim, 2013). So, the experimental value is closer to the literature values.

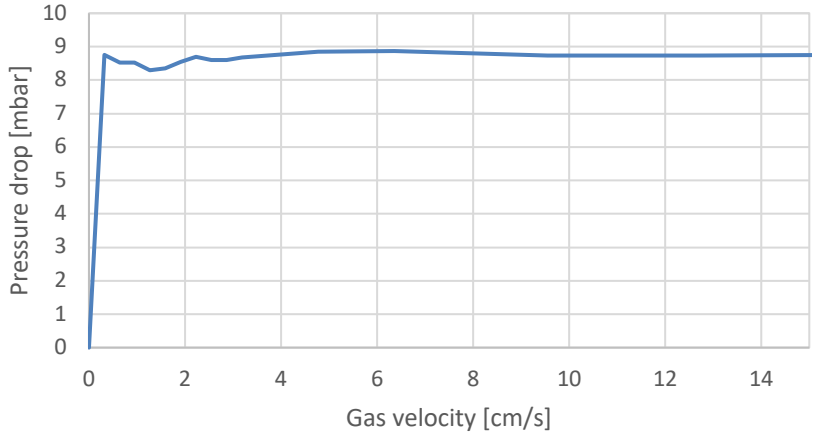

Figure 6.2 Secondary Alumina pressure profile

6.2.2 Filter dust

From Figure 5.4 it is difficult to obtain $U_{mf.}$ But from the experiments it can be observed visually as 0.63 cm/s (2 NLPM) when the whole bed started to move. And the exact U_t is hard to observe since smaller particles start to entrain at low velocities than expected. So, experimental U_t can be taken as 100 NLPM (31.51 cm/s). However, the theoretical U_{mf} and U_t are 0.934 cm/s and 42.813 cm/s respectively.

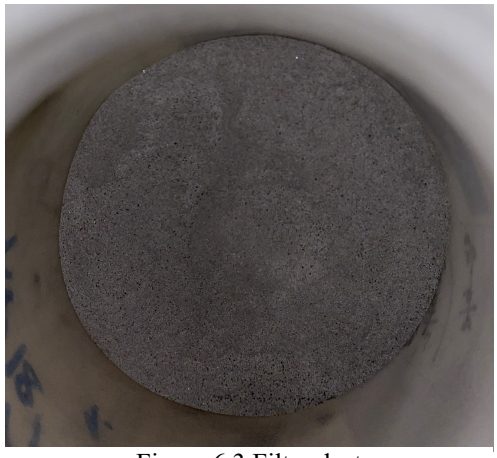

Figure 6.3 Filter dust

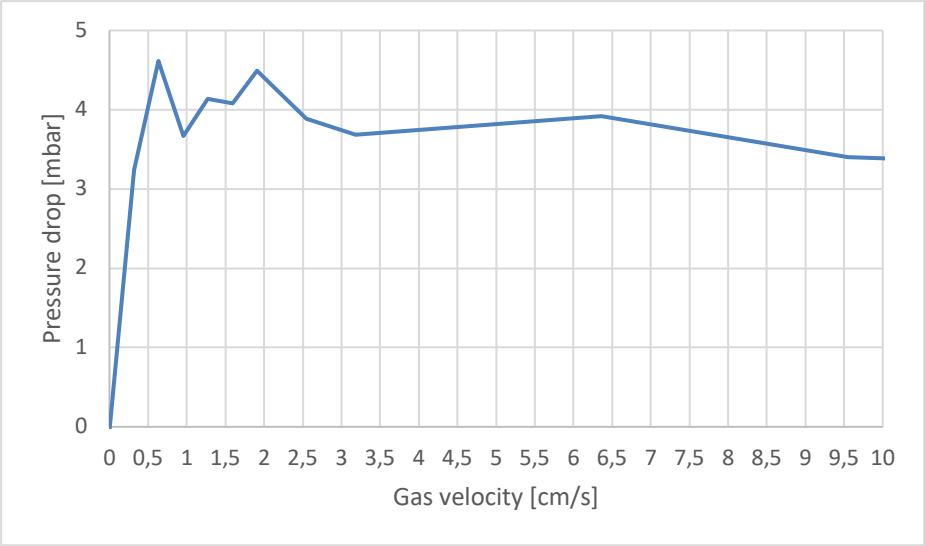

Figure 6.4 Filter dust pressure profile

6.2.3 Basement dust

Figure 5.6 shows the pressure drop profile for basement dust. Since it is difficult to obtain U_{mf} from the plot by visual observations it was around 1.26 cm/s (4 NLPM), and experimental U_t can be taken as 150 NLPM (47.27 cm/s). The theoretical U_{mf} and U_t are 1.145 cm/s and 55.42 cm/s respectively.

Figure 6.5 Basement dust

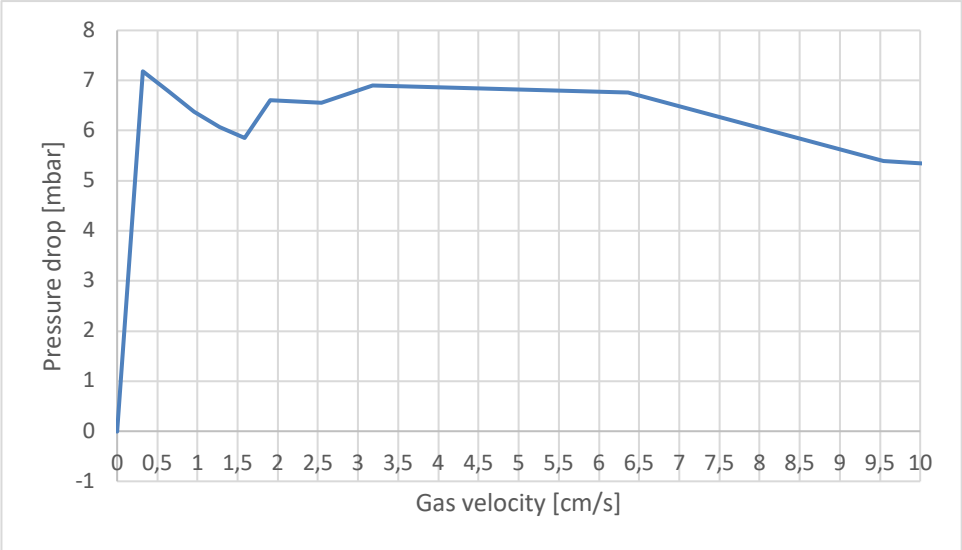

Figure 6.6 Basement dust pressure profile

Table 5.2 shows a comparison of experimental and calculated U_{mf} and U_t values for all the dust samples. And the calculated values were plotted against the corresponding experimental readings to present a validation of models used to calculate the respective velocities (Figure 5.7 and 5.8).

Table 6.2 Experimental vs. calculated values

	Secondary Alumina	Filter dust	Basement dust
d_p mean (um)	99.02	75.48	83.80
U_{mf} calculated (cm/s)	1.487	0.934	1.145
U_{mf} exp (cm/s)	1.10	0.63	1.26
U_t calculated (cm/s)	72.778	42.813	55.42
U_t exp (cm/s)	63.04	31.51	47.27

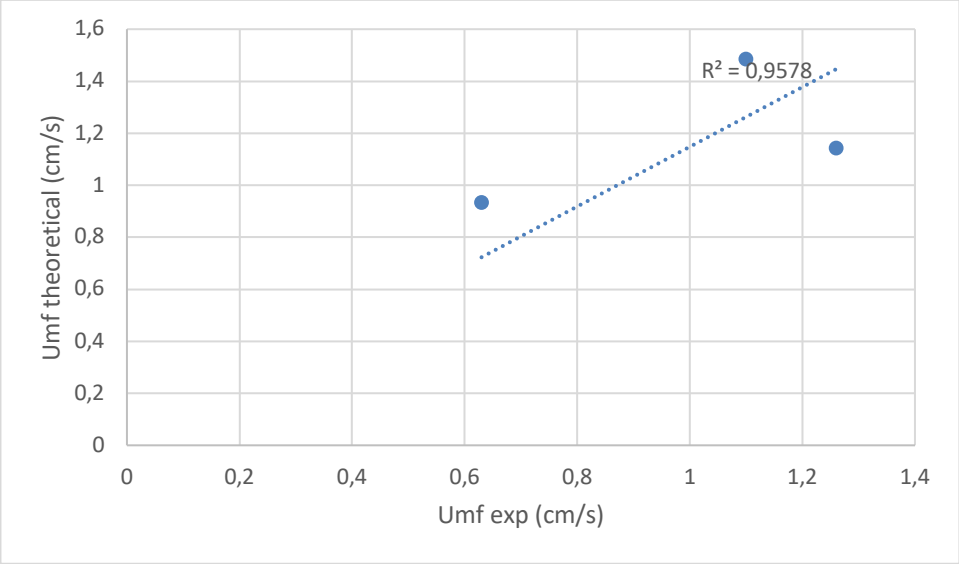

Figure 6.7 Experimental vs. calculated Umf

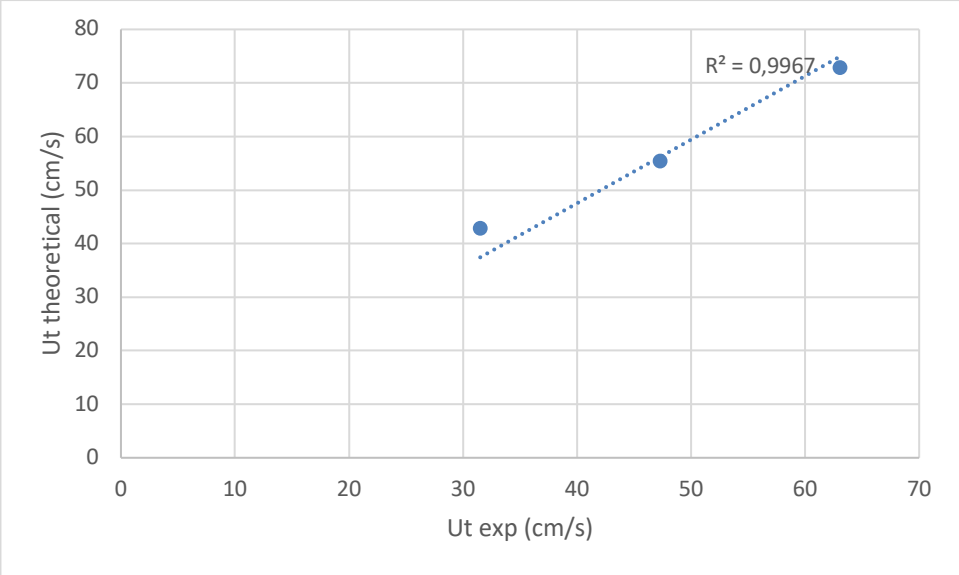

Figure 6.8 Experimental vs. calculated Ut

The calculated U_{mf} and U_t values were found to be in pretty good line with the experimental values as depicted in Figures 5.7 and 5.8. U_{mf} values show some visible variations than U_t values.

6.3 Binary mixture calculations

As explained in section 2.4 parameters for the binary mixtures were calculated as in Table 5.3.

Table 6.3 Parameters for binary mixtures

Mixture	Filter dust wt.%	Basement dust wt.%	$d_{p,mix}$ $[\mu m]$	ρ_{mix} [kg/m^3]	$\emptyset_{s,mix}$	U_{mf} [cm/s]	U_{mb} [cm/s]	U_t [cm/s]
M1	80	20	77.15	3493.44	0.68	0.673	0.06	41.851
M2	70	30	81.81	3505.87	0.78	0.760	0.942	48.89
M3	60	40	79.01	3498.41	0.72	0.07	0.921	44.342

There is no significant pattern in how the parameters change with the weight ratios. However, it can be observed that U_{mf}, U_{mb}, and U_t are highest in the M2 mixture.

6.4 Pneumatic system pressure drop

Table 5.4 shows the conveying system input data for binary mixtures at a solid conveying rate of 1 t/h. Calculations have done for 1 t/h and 2 t/h also for all the mixtures and the calculations were made in Excel. Gas inlet pressure was set to 2 bar initially, since at 1 bar the gas couldn't provide the required velocity to overcome choking at vertical flows.

Table 6.4 Conveying system input data

				M1	M2	M3
Type of conveying system		Pressure type				
Material to be conveyed		Filter dust + Basement dust				
Solid conveying rate	$\dot{m}_s$	1	t/h			
Pipe length	L	79	m			
Conveying pipe diameter	D	0.075	m			
Conveying pipe area	A	0.004417865	m^2			
Pipeline material		Steel				
Gravitational acceleration	g	9.81	m/s^2			
Gas used for conveying		Air				
Gas inlet temperature		25	C			

Gas inlet pressure		2×10^5	Pa			
Inlet gas density		2.34	kg/m^3			
Mean particle size weighted average			μm	77.15	81.81	79.01
Mixture density			kg/m^3	3493.44	3505.87	3498.41
Free fall velocity	w_{fo}		m/s	0.42	0.48	0.44
Minimum conveying velocity	v_{mcv}		m/s	8.29	8.30	8.29
Choking velocity in vertical flows	U_c		m/s	39.10	38.33	38.79
Solids mass velocity	W	62.88	kg/sm^2			
Solids loading ratio	μ	< 10 for dilute phase				
Solid additional pressure drop factor	λ_s	Depends on v_{cv}				

Table 5.5 depicts pipeline section data which consists of 15 sections; both straight pipe sections and bends together with equivalent lengths used in pressure drop calculations.

Table 6.5 Pipeline sections data

Section number	Pipeline component	Orientation	Length, m	Inside dimater, m	Section equivalent length, m	Cumulative equivalent length, m
1	Pipe	horizontal	6	0.075	6	6
2	90° Bend	horizontal to horizontal		0.075	12.192	18.192
3	Pipe	horizontal	21	0.075	21	39.192
4	90° Bend	horizontal to horizontal		0.075	12.192	51.384
5	Pipe	horizontal	13	0.075	13	64.384
6	90° Bend	horizontal to vertical		0.075	12.192	76.576
7	Pipe	vertical	8.25	0.075	8.25	84.826
8	90° Bend	vertical to horizontal		0.075	12.192	97.018
9	Pipe	horizontal	11	0.075	11	108.018
10	90° Bend	horizontal to vertical		0.075	12.192	120.21
11	Pipe	vertical	2.75	0.075	2.75	122.96
12	90° Bend	vertical to horizontal		0.075	12.192	135.152
13	Pipe	horizontal	10	0.075	10	145.152
14	90° Bend	horizontal to horizontal		0.075	12.192	157.344
15	Pipe	horizontal	7	0.075	7	164.344

	Total		79			

But for more accurate results the straight pipe sections were divided into 2 m small pipe sections and proceed the calculation accordingly. The updated pipeline section data is shown in Appendix C.

Appendix D shows a complete pressure drop calculation for M1 at a solid conveying rate of 1 t/h, an inlet pressure of 2 bar, and an inlet velocity of 30 m/s. The calculated minimum conveying velocity is 8.29 m/s and the choking velocity in vertical flows is 39.10 m/s for this mixture. To avoid particle blockage at vertical section 7, it is required to maintain the air velocity > 39.10 m/s. To provide these conditions the inlet velocity should be 30 m/s and the resultant pressure drop is 127427.12 Pa (~1.3 bar).

Table 6.6 Pressure drop: M1 with inlet air at 2 bar

$\dot{m}_s$	$\dot{m}_s$	v_{inlet}	$\dot{V}_a$	$\dot{m}_a$	$\mu = \frac{\dot{m}_s}{\dot{m}_a}$	v_{outlet}	$\Delta P = P_{inlet} - P_{outlet}$
t/h	kg/s	m/s	m^3/h	kg/s		m/s	Pa
1.0	0.278	30	0.133	0.310	0.896	85.63	127427.2
		32	0.141	0.331	0.840	125.19	147046.95
		34	0.150	0.351	0.790	316.19	177724.45
2.0	0.556	30	0.133	0.310	1.791	85.2	127667.96
		32	0.141	0.331	1.679	125.88	147336.35
		34	0.150	0.351	1.581	323.55	178230.9

If μ <10 (for dilute phase), then the assumed conveying velocity and pipe diameter is correct. In this study, the pipe dimensions remain constant, and optimize the pressure drop across the system while changing the inlet velocity. Therefore, changes in inlet velocity are more important. According to the data in Table 5.6, when the solid conveying rate is increased from 1 t/h to 2 t/h at a given inlet velocity, the pressure drop does not change significantly. When inlet velocity changes from 30 m/s to 34 m/s at a constant solid conveying rate, the pressure drop increases drastically, as well as the outlet velocity.

When the inlet air conditions change, it will also affect the pressure drop of the system by changing the minimum conveying velocity. Table 5.7 shows how inlet air pressure affects the system for M1 keeping the inlet air temperature constant at 25 ^{0}C throughout the system and at the minimum possible air velocity at 30 m/s. Hereafter the calculations will be performed only for a 1 t/h solid conveying rate since the solid conveying rate does not play a significant role in the optimization process.

Table 6.7 Pressure drop: M1 with different inlet air pressures

$P_{initial}$	$\rho_{a,initial}$	v_{mcv}	U_c	v_{inlet}	v_{outlet}	$\Delta P = P_{inlet} - P_{outlet}$
bar	kg/m^3	m/s	m/s	m/s	m/s	Pa
2	2.34	8.29	39.10	30	73.47	127427.12
3	3.51	6.77	25.18	22	29.86	71032.16
4	4.67	5.87	18.51	18	21.54	54522.70

As inlet air pressure increases, the minimum conveying velocity decreases from 8.29 m/s to 5.87 m/s, while the choking velocity in vertical flows decreases from 39.10 m/s to 18.51 m/s. As a result, the required air velocity to convey this M1 mixture will decrease from 30 m/s to 18 m/s. The system pressure drop has been reduced as well from 127427.12 Pa (1.28 bar) to 54522.70 Pa (0.54 bar).

In this study three different mixtures were considered: M1, M2, and M3. Table 5.4 shows the variation of a few parameters for the mixtures at 1 t/h solid conveying rate. One of the main objectives of this study was to examine the behavior of the mixtures with different mass ratios of filter dust and basement dust, hence optimizing the pneumatic conveying system. Therefore Table 5.8 summarizes a comparison of parameters that are vital for system optimization.

Table 6.8 Comparison of mixtures

$P_{initial}$	Pa	2×10^5			3×10^5			4×10^5		
		M1	M2	M3	M1	M2	M3	M1	M2	M3
v_{mcv}	m/s	8.29	8.30	8.29	6.77	6.78	6.77	5.87	5.88	5.87
U_c	m/s	39.10	38.33	38.79	25.18	24.71	24.99	18.51	18.18	18.37
$v_{initial}$	m/s	30			22			18		
ΔP	Pa	127427.12			71032.16			54522.70		

As per Table 5.8, it can be said that the effect of the mass ratio of filter dust and basement dust on the system pressure drop is negligible. Since the minimum conveying velocities and choking velocities are almost the same for a given mixture. Therefore, conveying velocity can be set to a constant value for all the mixtures at a given initial air pressure. So, the system pressure drop basically depends on initial air conditions, i.e., air pressure and inlet velocity.

In a pneumatic conveying system, the conveying air velocity is an important parameter that influences the material flow rate, pressure drop, and power consumption. To achieve efficient and reliable material transportation, the conveying air velocity must be properly chosen. Generally, the conveying velocity should be high enough to prevent material from settling in the pipeline, but not so high that the pipeline undergoes excessive wear and erosion. Industries

use 15-20 m/s for dilute phase pneumatic conveying and 3-8 m/s for dense phase pneumatic conveying as a rule of thumb (IAC, 2022).

Therefore, the selected initial conveying velocities are reliable for the system in this study. Once the conveying air velocity has been determined, it must be validated with experimental studies to ensure reliable and efficient material conveyance. The conveying air velocity may need to be adjusted based on the testing findings and the material and system's specific characteristics.

Several factors contribute to pressure drop in a dilute phase pneumatic conveying system, including frictional losses, acceleration, and changes in direction or elevation. Understanding how these factors contribute to pressure drop might help find areas for optimization. The particle characteristics, such as particle size, shape, and density affect the pressure drop. To ensure that the pressure drop calculation is as precise as possible, accurate material characteristics should be used. The pipeline dimensions also significantly impact the pressure drop. So, careful selection of pipeline diameter and conveying distance to minimize pressure drop is important. Also, the pipeline layout including a less number of bends and fewer changes in direction and elevation can reduce the pressure drop (Ratnayake, 2005).

Because of changes in material characteristics, pipeline fouling, or other variables, the pressure drop in a dilute phase pneumatic conveying system may change over time. Continuously monitoring and optimizing the system is needed to ensure a reliable operation.

Conclusion

At one of Hydro's Aluminium plants dusting in the crushing and storage area of the anode cover material plant has been identified as an environmental issue that requires further work and retrofit of existing bulk solids handling equipment and logistics. The source of dusting has been identified as coming from uncontrolled mixing of two material flows: filter and potroom basement dust. The two materials are two of the ingredients of anode cover material (ACM for potrooms. ACM quality has not been a key performance indicator (KPI) for the Aluminium plants, focus is on quantity, that is, to have enough ACM material in the main silos to cover the anodes.

This study has investigated theoretical approach of designing a pneumatic conveying system to handle mixtures of the two flows of material, in order to have a cleaner working environment in the crushing and storage area of the ACM plant. If information about the plant in terms of variations, where and why the variations occur is not accurate or missing, implementation of any transport system will be wasted as the current situation clearly shows it. That is why, the most anti-dusting and quality control tools one has is characterization of bulk property of the materials. It is strange, and a valuable experience for any newly educated engineer to keep in mind, that a plant will invest in control systems, laboratory equipment and other expensive control methods, but when designing and installing the bulk handling systems, one fails in identifying and mixing the different ingredients properly.

To conclude the findings of this study, it can be said that for a design of a pneumatic conveying system, the most important parameters will be the initial gas pressure and initial conveying velocity. For a given solid conveying rate with fixed pipeline configuration, the system pressure drop decreases as the initial gas pressure increases and it needs lower conveying velocities as the minimum required conveying velocity decreases. In this study, the pressure drop is not affected by the mixture composition. It depends only on initial gas pressure and initial gas velocity. Initial velocities for all three mixtures can be set to a fixed value because the minimum conveying velocities and choking velocities are almost the same. To help in choosing the proper design parameters for a system it is required to perform pilot testing and validate the parameters. Therefore, the excel work sheet which has generated for this study can be used for further experiments to optimize the design parameters for a full-scale conveying system design. A dilute phase conveying system's energy consumption is greatly affected by air velocity. Also, high pressure can result in degradation of materials and leaks wasting energy. In this study it is difficult to optimize the power consumption based on mixture ratios. The mixture ratios are not in a wide range, so they are not having a high impact on the system. After designing the system and choosing the parameters, the system can be improved in terms of performance and energy efficiency with regular monitoring and maintenance.

Future work and recommendations

Alumina and the anode cover material (ACM) are stored at main storage sites, conveyed to buffer and main silos, stored, and passed through the crushing and fume treatment plant, stored in buffer silos for secondary alumina, distributed to the pots by pneumatic conveying or air slides and finally fed to the pots and used as anode covering. One may see that logistics, process, and working operations, as well as the environment, are interdependent, interacting all the way. The sampling campaign carried out as the basis for this work has been a compromise of accessibility, extent of work, and of course costs. The costs would have been much smaller if proper knowledge, sampling points, mixing of materials, and optimized logistics had been embedded in the design of the plant to begin with. The system needs to supply a constant fed of material to the process in order to make it stable, thus less operator intervention, hence less exposure for operators to heat, dust and gases. As a result, the total emissions of gases and dust to the working environment and to the atmosphere will be reduced. Environmental demands from the government and the public (stakeholders around the plants, e.g., farmers, households, and animals) enforce the need for an optimized design and a controlled interaction between the Aluminium production and raw material handling.

Due to insufficient time pressure drop calculations in this study were solely based on theoretical studies which used mathematical models from literature. Pilot trials with different mixture compositions under controllable conditions with the installed pneumatic conveying system at Powder Hall can assist to validate the theoretical calculations and ensure the system functions as predicted.

Certain general design considerations in pneumatic conveying systems are generally not found in the usual literature but come from extensive field experience (de Silva, n.d.). When designing a conveying system, the most direct route from the feeder to the delivery point with the fewest bends in the system is preferred. When installing piping, it is essential that the pipes remain aligned. Pipes that are misaligned will tend to erode the piping. Any sort of wear-back bend, including the conventional T-bend, is recommended for system durability.

References

Aarhaug, T. A., & Ratvik, A. P. (2019). Aluminium Primary Production Off-Gas Composition and Emissions: An Overview. *JOM*, *71*(9), 2966–2977. https://doi.org/10.1007/s11837-019-03370-6

Agarwal, A. T. (2005). *Theory and Design of Dilute Phase Pneumatic Conveying Systems*. *17*.

Anantharaman, A., Cahyadi, A., Hadinoto, K., & Chew, J. W. (2016). Impact of particle diameter, density and sphericity on minimum pickup velocity of binary mixtures in gas-solid pneumatic conveying. *Powder Technology*, *297*, 311–319. https://doi.org/10.1016/j.powtec.2016.04.038

Are Dyroy 2006—Redacted.pdf. (n.d.).

de Silva, S. R. (n.d.). *TRANSPORT OF PARTICULATE MATERIALS- Dilute Phase Pneumatic Transport*.

Dechsiri, C. (2004). *Particle Transport in Fluidized Beds: Experiments and Stochastic Models*. University of Groningen. https://.rug.nl/en/publications/particle-transport-in-fluidized-beds-experiments-and-stochastic-m

Dhodapkar, S., & Cocco, R. (2022, March 24). *Basic concepts in pneumatic conveying*. https://www.processingmagazine.com/material-handling-dry-wet/conveyors/pneumatic---vacuum/article/21258145/basic-concepts-in-pneumatic-conveying

Geldart, D. (1973). Types of gas fluidization. *Powder Technology*, *7*(5), 285–292. https://doi.org/10.1016/0032-5910(73)80037-3

Haider, A., & Levenspiel, O. (1989). Drag coefficient and terminal velocity of spherical and nonspherical particles. *Powder Technology*, *58*(1), 63–70. https://doi.org/10.1016/0032-5910(89)80008-7

Kunii, D., & Levenspiel, O. (2012). *Fluidization engineering* (2. ed., reprinted). Elsevier ; Butterworth-Heinemann.

MP-20-22.pdf. (n.d.).

Naveh, R., Tripathi, N. M., & Kalman, H. (2017). *Experimental pressure drop analysis for horizontal dilute phase particle-fluid flows, Powder Technology* (Vol. 321).

Niven, R. K. (2002). Physical insight into the Ergun and Wen & Yu equations for fluid flow in packed and fluidised beds. *Chemical Engineering Science*, *57*(3), 527–534. https://doi.org/10.1016/S0009-2509(01)00371-2

Norheim, K. (2013). *Fluidisation tester*. Hydro.

PowderProcess. (n.d.). *Minimum air conveying velocity Pick-up speed*. https://powderprocess.net/Pneumatic_Transport/Pick_Up_Velocity.html

Ratnayake, C. (2005). *A Comprehensive Scaling Up Technique for Pneumatic Transport Systems*. https://www.researchgate.net/publication/37686963_A_comprehensive_scaling_up_technique_for_pneumatic_transport_systems

Serena Carmen Valciu 2015.pdf. (n.d.).

Weber, M. (1982). *Correlation Analyses in the Design of Pneumatic Transport Plant. Bulk Solids Handling: Vol. 2(2)*.

Woodcock, C. R., & Mason, J. S. (1987). *Bulk Solids Handling—An Introduction to the Practice and Technology*.

Wypych, P. W., & Arnold, P. C. (1987). *On Improving Scale-up Procedures for Pneumatic Conveying Design. Powder Technology* (Vol. 1–50(3)).

Yang, W. (1975). *A mathematical definition of choking phenomenon and a mathematical model for predicting choking velocity and choking voidage*. https://www.semanticscholar.org/paper/A-mathematical-definition-of-choking-phenomenon-and-Yang/f23987c57469f58e0274d2f0f0b7bfe0b7a27304

Zenz, & Othmer. (1960). *Fluidized and Fluid Particle Systems*. Reinhold Publishing Corporation, New York, NY.

https://iac-intl.com/oem-engineered-systems/pneumatic-conveying-systems/dilute-phase-conveying/#:~:text=Material%20is%20suspended%20in%20the,ft%2Fmin%20for%20heavier%20materials.

Appendices

Appendix A

Minimum fluidization velocity and Minimum bubbling velocity

A-1: Secondary alumina

d_p (μm)	cumm wt.%	wt.%	d_p*wt.%	d_p mean (μm)	U_{mf} (cm/s)	U_{mf}*wt.%	U_{mf} mean (cm/s)	Re_{mf}	U_{mb} (cm/s)	U_{mb}*wt.%	U_{mb} mean (cm/s)
1,8	0,6	0,6	0,011	99,015	0,0004	2,3785E-06	1,4865	4,6668E-07	0,0183	1,0995E-04	1,0081
2,2	0,73	0,13	0,003		0,0006	7,6983E-07		8,5205E-07	0,0224	2,9118E-05	
2,6	0,84	0,11	0,003		0,0008	9,0980E-07		1,4064E-06	0,0265	2,9118E-05	
3	0,94	0,1	0,003		0,0011	1,1012E-06		2,1605E-06	0,0305	3,0543E-05	
3,6	1,07	0,13	0,005		0,0016	2,0614E-06		3,7334E-06	0,0367	4,7647E-05	
4,4	1,23	0,16	0,007		0,0024	3,7899E-06		6,8164E-06	0,0448	7,1674E-05	
5,2	1,36	0,13	0,007		0,0033	4,3009E-06		1,1251E-05	0,0529	6,8823E-05	
6,2	1,52	0,16	0,010		0,0047	7,5250E-06		1,9071E-05	0,0631	1,0100E-04	
7,4	1,71	0,19	0,014		0,0067	1,2730E-05		3,2426E-05	0,0753	1,4314E-04	
8,6	1,9	0,19	0,016		0,0090	1,7193E-05		5,0897E-05	0,0876	1,6636E-04	
10	2,13	0,23	0,023		0,0122	2,8141E-05		8,0020E-05	0,1018	2,3416E-04	
12	2,48	0,35	0,042		0,0176	6,1665E-05		1,3827E-04	0,1222	4,2760E-04	
15	3,05	0,57	0,086		0,0275	1,5691E-04		2,7007E-04	0,1527	8,7047E-04	

18	3,66	0,61	0,110		0,0396	2,4181E-04		4,6668E-04	0,1833	1,1179E-03	
21	4,33	0,67	0,141		0,0540	3,6151E-04		7,4106E-04	0,2138	1,4325E-03	
25	5,34	1,01	0,253		0,0765	7,7234E-04		1,2503E-03	0,2545	2,5707E-03	
30	6,84	1,5	0,450		0,1101	1,6517E-03		2,1605E-03	0,3054	4,5814E-03	
36	9,09	2,25	0,810		0,1586	3,5677E-03		3,7334E-03	0,3665	8,2466E-03	
42	11,94	2,85	1,197		0,2158	6,1510E-03		5,9285E-03	0,4276	1,2187E-02	
50	16,8	4,86	2,430		0,3059	1,4866E-02		1,0002E-02	0,5090	2,4740E-02	
60	24,48	7,68	4,608		0,4405	3,3827E-02		1,7284E-02	0,6109	4,6914E-02	
72	35,37	10,89	7,841		0,6343	6,9071E-02		2,9867E-02	0,7330	7,9827E-02	
86	48,91	13,54	11,644		0,9049	1,2252E-01		5,0897E-02	0,8756	1,1855E-01	
102	63,76	14,85	15,147		1,2729	1,8903E-01		8,4918E-02	1,0385	1,5421E-01	
122	78,83	15,07	18,385		1,8211	2,7443E-01		1,4530E-01	1,2421	1,8718E-01	
146	90,09	11,26	16,440		2,6080	2,9366E-01		2,4903E-01	1,4864	1,6737E-01	
174	96,2	6,11	10,631		3,7043	2,2633E-01		4,2155E-01	1,7715	1,0824E-01	
206	98,6	2,4	4,944		5,1921	1,2461E-01		6,9952E-01	2,0973	5,0335E-02	
246	99,49	0,89	2,189		7,4042	6,5897E-02		1,1913E+00	2,5045	2,2290E-02	
294	99,88	0,39	1,147		10,5755	4,1244E-02		2,0335E+00	2,9932	1,1674E-02	
350	100	0,12	0,420		14,9879	1,7986E-02		3,4309E+00	3,5633	4,2760E-03	

A-2: Filter dust

d_p (μm)	cumm wt.%	wt.%	d_p*wt.%	d_p mean (μm)	U_{mf} (cm/s)	U_{mf}*wt.%	U_{mf} mean (cm/s)	Re_{mf}	U_{mb} (cm/s)	U_{mb}*wt.%	U_{mb} mean (cm/s)
1,8	1,76	1,76	0,032	75,481	0,0004	6,4447E-06	0,9340	4,3108E-07	0,0213	3,7487E-04	0,8932
2,2	2,26	0,5	0,011		0,0005	2,7350E-06		7,8706E-07	0,0260	1,3016E-04	
2,6	2,74	0,48	0,012		0,0008	3,6672E-06		1,2992E-06	0,0308	1,4767E-04	
3	3,21	0,47	0,0141		0,0010	4,7807E-06		1,9957E-06	0,0355	1,6684E-04	
3,6	3,89	0,68	0,024		0,0015	9,9601E-06		3,4486E-06	0,0426	2,8967E-04	
4,4	4,74	0,85	0,037		0,0022	1,8598E-05		6,2965E-06	0,0521	4,4255E-04	
5,2	5,56	0,82	0,043		0,0031	2,5059E-05		1,0393E-05	0,0615	5,0455E-04	
6,2	6,53	0,97	0,060		0,0043	4,2141E-05		1,7616E-05	0,0734	7,1163E-04	
7,4	7,64	1,11	0,082		0,0062	6,8696E-05		2,9953E-05	0,0876	9,7195E-04	
8,6	8,71	1,07	0,092		0,0084	8,9439E-05		4,7015E-05	0,1018	1,0889E-03	
10	9,91	1,2	0,120		0,0113	1,3562E-04		7,3916E-05	0,1183	1,4199E-03	
12	11,59	1,68	0,202		0,0163	2,7341E-04		1,2773E-04	0,1420	2,3855E-03	
15	14,05	2,46	0,369		0,0254	6,2556E-04		2,4947E-04	0,1775	4,3663E-03	
18	16,48	2,43	0,437		0,0366	8,8981E-04		4,3108E-04	0,2130	5,1757E-03	
21	18,88	2,4	0,504		0,0498	1,1962E-03		6,8454E-04	0,2485	5,9638E-03	
25	22,01	3,13	0,783		0,0706	2,2109E-03		1,1549E-03	0,2958	9,2592E-03	
30	25,75	3,74	1,122		0,1017	3,8042E-03		1,9957E-03	0,3550	1,3276E-02	

36	29,92	4,17	1,501		0,1465	6,1079E-03		3,4486E-03	0,4260	1,7764E-02	
42	33,78	3,86	1,621		0,1994	7,6954E-03		5,4763E-03	0,4970	1,9183E-02	
50	38,74	4,96	2,480		0,2825	1,4014E-02		9,2395E-03	0,5916	2,9346E-02	
60	45,19	6,45	3,870		0,4069	2,6243E-02		1,5966E-02	0,7100	4,5793E-02	
72	53,68	8,49	6,113		0,5859	4,9742E-02		2,7589E-02	0,8520	7,2332E-02	
86	64,27	10,59	9,107		0,8359	8,8520E-02		4,7015E-02	1,0176	1,0777E-01	
102	75,71	11,44	11,669		1,1758	1,3452E-01		7,8441E-02	1,2070	1,3808E-01	
122	86,8	11,09	13,530		1,6822	1,8655E-01		1,3422E-01	1,4436	1,6010E-01	
146	94,46	7,66	11,184		2,4091	1,8454E-01		2,3004E-01	1,7276	1,3233E-01	
174	98,12	3,66	6,368		3,4217	1,2524E-01		3,8939E-01	2,0589	7,5356E-02	
206	99,45	1,33	2,740		4,7960	6,3787E-02		6,4616E-01	2,4376	3,2420E-02	
246	100	0,55	1,353		6,8394	3,7617E-02		1,1004E+00	2,9109	1,6010E-02	
294	100	0	0,000		9,7688	0,0000E+00		1,8784E+00	3,4789	0,0000E+00	
350	100	0	0,000		13,8447	0,0000E+00		3,1692E+00	4,1415	0,0000E+00	

A-3: Basement dust

d_p (μm)	cumm wt.%	wt.%	d_p*wt.%	d_p mean (μm)	U_{mf} (cm/s)	U_{mf}*wt.% (cm/s)	U_{mf} mean (cm/s)	Re_{mf}	U_{mb} (cm/s)	U_{mb}*wt.%	U_{mb} mean (cm/s)
1,8	1,28	1,28	0,023	83,804	0,0004	8,4905E-06	1,1453	4,3382E-07	0,0206	2,6304E-02	0,9568
2,2	1,63	0,35	0,008		0,0006	4,2388E-06		7,9207E-07	0,0251	8,7909E-03	
2,6	1,95	0,32	0,008		0,0008	6,3970E-06		1,3074E-06	0,0297	9,4987E-03	

3	2,26	0,31	0,0093		0,0010	9,5198E-06		2,0084E-06	0,0343	1,0618E-02	
3,6	2,69	0,43	0,015		0,0015	2,2818E-05		3,4706E-06	0,0411	1,7673E-02	
4,4	3,22	0,53	0,023		0,0022	5,1350E-05		6,3366E-06	0,0502	2,6624E-02	
5,2	3,72	0,5	0,026		0,0031	7,9962E-05		1,0459E-05	0,0594	2,9684E-02	
6,2	4,31	0,59	0,037		0,0044	1,5993E-04		1,7728E-05	0,0708	4,1762E-02	
7,4	4,97	0,66	0,049		0,0062	3,0419E-04		3,0143E-05	0,0845	5,5759E-02	
8,6	5,62	0,65	0,056		0,0084	4,7023E-04		4,7314E-05	0,0982	6,3820E-02	
10	6,37	0,75	0,075		0,0114	8,5303E-04		7,4387E-05	0,1142	8,5626E-02	
12	7,45	1,08	0,130		0,0164	2,1226E-03		1,2854E-04	0,1370	1,4796E-01	
15	9,08	1,63	0,245		0,0256	6,2570E-03		2,5106E-04	0,1713	2,7914E-01	
18	10,71	1,63	0,293		0,0369	1,0812E-02		4,3382E-04	0,2055	3,3497E-01	
21	12,36	1,65	0,347		0,0502	1,7380E-02		6,8890E-04	0,2398	3,9559E-01	
25	14,62	2,26	0,565		0,0711	4,0164E-02		1,1623E-03	0,2854	6,4505E-01	
30	17,64	3,02	0,906		0,1024	9,2742E-02		2,0084E-03	0,3425	1,0344E+00	
36	21,62	3,98	1,433		0,1474	2,1120E-01		3,4706E-03	0,4110	1,6358E+00	
42	26,03	4,41	1,852		0,2006	3,7161E-01		5,5112E-03	0,4795	2,1146E+00	
50	32,46	6,43	3,215		0,2843	9,1416E-01		9,2984E-03	0,5708	3,6705E+00	
60	41,02	8,56	5,136		0,4095	2,1030E+00		1,6068E-02	0,6850	5,8636E+00	
72	51,44	10,42	7,502		0,5896	4,4235E+00		2,7765E-02	0,8220	8,5653E+00	
86	62,96	11,52	9,907		0,8412	8,3340E+00		4,7314E-02	0,9818	1,1311E+01	

102	74,2	11,24	11,465		1,1833	1,3567E+01		7,8940E-02	1,1645	1,3089E+01	
122	84,42	10,22	12,468		1,6929	2,1107E+01		1,3508E-01	1,3928	1,4235E+01	
146	91,54	7,12	10,395		2,4244	2,5202E+01		2,3150E-01	1,6668	1,1868E+01	
174	95,51	3,97	6,908		3,4435	2,3787E+01		3,9187E-01	1,9865	7,8865E+00	
206	97,59	2,08	4,285		4,8266	2,0681E+01		6,5028E-01	2,3518	4,8918E+00	
246	98,97	1,38	3,395		6,8829	2,3366E+01		1,1074E+00	2,8085	3,8758E+00	
294	100	1,03	3,028		9,8310	2,9770E+01		1,8903E+00	3,3565	3,4572E+00	
350	100	0	0,000		13,9328	0,0000E+00		3,1893E+00	3,9959	0,0000E+00	

Appendix B

Terminal settling velocity

B-1: Secondary alumina

d_p (μm)	cumm wt.%	wt.%	d_p*	U_t*	U_t (cm/s)	U_t*wt.%	U_t mean (cm/s)
1,8	0,6	0,6	0,0917	0,0005	0,0363	2,1774E-04	72,7782
2,2	0,73	0,13	0,1120	0,0007	0,0542	7,0439E-05	
2,6	0,84	0,11	0,1324	0,0010	0,0756	8,3204E-05	
3	0,94	0,1	0,1528	0,0013	0,1006	1,0065E-04	
3,6	1,07	0,13	0,1833	0,0019	0,1448	1,8824E-04	
4,4	1,23	0,16	0,2241	0,0028	0,2160	3,4563E-04	
5,2	1,36	0,13	0,2648	0,0039	0,3013	3,9166E-04	
6,2	1,52	0,16	0,3157	0,0055	0,4274	6,8391E-04	
7,4	1,71	0,19	0,3768	0,0078	0,6073	1,1539E-03	
8,6	1,9	0,19	0,4379	0,0105	0,8180	1,5542E-03	
10	2,13	0,23	0,5092	0,0142	1,1021	2,5349E-03	
12	2,48	0,35	0,6110	0,0203	1,5784	5,5245E-03	
15	3,05	0,57	0,7638	0,0314	2,4443	1,3932E-02	
18	3,66	0,61	0,9166	0,0448	3,4854	2,1261E-02	
21	4,33	0,67	1,0693	0,0603	4,6941	3,1451E-02	
25	5,34	1,01	1,2730	0,0842	6,5529	6,6184E-02	
30	6,84	1,5	1,5276	0,1188	9,2467	1,3870E-01	

36	9,09	2,25	1,8331	0,1666	12,9727	2,9189E-01	
42	11,94	2,85	2,1387	0,2206	17,1769	4,8954E-01	
50	16,8	4,86	2,5460	0,3008	23,4211	1,1383E+00	
60	24,48	7,68	3,0552	0,4118	32,0655	2,4626E+00	
72	35,37	10,89	3,6663	0,5570	43,3668	4,7226E+00	
86	48,91	13,54	4,3792	0,7374	57,4154	7,7740E+00	
102	63,76	14,85	5,1939	0,9519	74,1124	1,1006E+01	
122	78,83	15,07	6,2123	1,2242	95,3115	1,4363E+01	
146	90,09	11,26	7,4344	1,5479	120,5149	1,3570E+01	
174	96,2	6,11	8,8602	1,9129	148,9373	9,1001E+00	
206	98,6	2,4	10,4897	2,3079	179,6866	4,3125E+00	
246	99,49	0,89	12,5265	2,7661	215,3601	1,9167E+00	
294	99,88	0,39	14,9707	3,2671	254,3715	9,9205E-01	
350	100	0,12	17,8222	3,7938	295,3784	3,5445E-01	

B-2: Filter dust

d_p (μm)	cumm wt.%	wt.%	d_p*	U_t*	U_t (cm/s)	U_t*wt.%	U_t mean (cm/s)
1,8	1,76	1,76	0,0893	0,0004	0,0335	5,8972E-04	42,8127
2,2	2,26	0,5	0,1091	0,0007	0,0500	2,5011E-04	
2,6	2,74	0,48	0,1289	0,0009	0,0698	3,3512E-04	
3	3,21	0,47	0,1488	0,0012	0,0929	4,3655E-04	

3,6	3,89	0,68	0,1785	0,0018	0,1336	9,0842E-04	
4,4	4,74	0,85	0,2182	0,0026	0,1992	1,6933E-03	
5,2	5,56	0,82	0,2579	0,0037	0,2777	2,2771E-03	
6,2	6,53	0,97	0,3075	0,0052	0,3937	3,8193E-03	
7,4	7,64	1,11	0,3670	0,0074	0,5590	6,2048E-03	
8,6	8,71	1,07	0,4265	0,0099	0,7522	8,0486E-03	
10	9,91	1,2	0,4959	0,0134	1,0123	1,2148E-02	
12	11,59	1,68	0,5951	0,0191	1,4474	2,4316E-02	
15	14,05	2,46	0,7439	0,0295	2,2350	5,4981E-02	
18	16,48	2,43	0,8926	0,0419	3,1773	7,7208E-02	
21	18,88	2,4	1,0414	0,0563	4,2653	1,0237E-01	
25	22,01	3,13	1,2398	0,0782	5,9273	1,8552E-01	
30	25,75	3,74	1,4877	0,1096	8,3141	3,1095E-01	
36	29,92	4,17	1,7853	0,1527	11,5778	4,8280E-01	
42	33,78	3,86	2,0828	0,2006	15,2138	5,8725E-01	
50	38,74	4,96	2,4796	0,2708	20,5334	1,0185E+00	
60	45,19	6,45	2,9755	0,3661	27,7589	1,7904E+00	
72	53,68	8,49	3,5706	0,4879	36,9971	3,1411E+00	
86	64,27	10,59	4,2649	0,6357	48,2033	5,1047E+00	
102	75,71	11,44	5,0583	0,8070	61,1885	7,0000E+00	

122	86,8	11,09	6,0502	1,0188	77,2476	8,5668E+00	
146	94,46	7,66	7,2404	1,2640	95,8431	7,3416E+00	
174	98,12	3,66	8,6289	1,5339	116,3113	4,2570E+00	
206	99,45	1,33	10,2159	1,8200	138,0039	1,8355E+00	
246	100	0,55	12,1995	2,1463	162,7474	8,9511E-01	
294	100	0	14,5799	2,4986	189,4565	0,0000E+00	
350	100	0	17,3571	2,8657	217,2936	0,0000E+00	

B-3: Basement dust

d_p (μm)	cumm wt.%	wt.%	d_p*	U_t*	U_t (cm/s)	U_t*wt.%	U_t mean (cm/s)
1,8	1,28	1,28	0,0895	0,0004	0,0337	4,3181E-04	55,4207
2,2	1,63	0,35	0,1093	0,0007	0,0504	1,7630E-04	
2,6	1,95	0,32	0,1292	0,0009	0,0703	2,2502E-04	
3	2,26	0,31	0,1491	0,0012	0,0936	2,9006E-04	
3,6	2,69	0,43	0,1789	0,0018	0,1346	5,7885E-04	
4,4	3,22	0,53	0,2187	0,0026	0,2008	1,0644E-03	
5,2	3,72	0,5	0,2584	0,0037	0,2801	1,4005E-03	
6,2	4,31	0,59	0,3081	0,0052	0,3974	2,3447E-03	
7,4	4,97	0,66	0,3678	0,0074	0,5647	3,7270E-03	
8,6	5,62	0,65	0,4274	0,0100	0,7606	4,9438E-03	
10	6,37	0,75	0,4970	0,0135	1,0248	7,6862E-03	

12	7,45	1,08	0,5964	0,0193	1,4679	1,5853E-02	
15	9,08	1,63	0,7454	0,0299	2,2734	3,7057E-02	
18	10,71	1,63	0,8945	0,0427	3,2422	5,2848E-02	
21	12,36	1,65	1,0436	0,0575	4,3674	7,2061E-02	
25	14,62	2,26	1,2424	0,0803	6,0982	1,3782E-01	
30	17,64	3,02	1,4909	0,1133	8,6077	2,5995E-01	
36	21,62	3,98	1,7891	0,1590	12,0810	4,8082E-01	
42	26,03	4,41	2,0873	0,2106	16,0027	7,0572E-01	
50	32,46	6,43	2,4848	0,2873	21,8320	1,4038E+00	
60	41,02	8,56	2,9818	0,3936	29,9103	2,5603E+00	
72	51,44	10,42	3,5782	0,5328	40,4846	4,2185E+00	
86	62,96	11,52	4,2739	0,7060	53,6475	6,1802E+00	
102	74,2	11,24	5,0691	0,9122	69,3148	7,7910E+00	
122	84,42	10,22	6,0630	1,1744	89,2371	9,1200E+00	
146	91,54	7,12	7,2557	1,4866	112,9605	8,0428E+00	
174	95,51	3,97	8,6472	1,8392	139,7543	5,5482E+00	
206	97,59	2,08	10,2375	2,2212	168,7804	3,5106E+00	
246	98,97	1,38	12,2254	2,6649	202,4932	2,7944E+00	
294	100	1,03	14,6108	3,1505	239,3944	2,4658E+00	
350	100	0	17,3938	3,6613	278,2083	0,0000E+00	

Appendix C

Pipeline section data

Section number	Pipeline component	Orientation	Length, m	Inside dimater, m	Section equivalent length, m	Cumulative equivalent length, m
1	pipe	horizontal	2	0,075	2	
			2		2	
			2		2	6
2	90 ° Bend	horizontal to horizontal		0,075	12,192	18,192
3	pipe	horizontal	2	0,075	2	
			2		2	
			2		2	
			2		2	
			2		2	
			2		2	
			2		2	
			2		2	
			2		2	
			2		2	
			1		1	39,192
4	90 ° Bend	horizontal to horizontal		0,075	12,192	51,384
5	pipe	horizontal	2	0,075	2	
			2		2	
			2		2	
			2		2	
			2		2	

			2		2	
			1		1	64,384
6	90 ° Bend	horizontal to vertical		0,075	12,192	76,576
7	pipe	vertical	2	0,075	2	
			2		2	
			2		2	
			2		2	
			0,25		0,25	84,826
8	90 ° Bend	vertical to horizontal		0,075	12,192	97,018
9	pipe	horizontal	2	0,075	2	
			2		2	
			2		2	
			2		2	
			2		2	
			1		1	108,018
10	90 ° Bend	horizontal to vertical		0,075	12,192	120,21
11	pipe	vertical	2	0,075	2	
			0,75		0,75	122,96
12	90 ° Bend	vertical to horizontal			12,192	135,152
13	pipe	horizontal	2		2	
			2		2	
			2		2	
			2		2	
			2		2	145,152
14	90 ° Bend	horizontal to horizontal		0,075	12,192	157,344
15	pipe	horizontal	2	0,075	2	
			2		2	

			2		2	
			1		1	164,344
	total		79			

Appendix D

Pressure drop calculations

M1 at solid conveying rate = 1 t/h and initial pressure = 2 bar

Section Number	pressure drop in each section, Pa							gas temperature	inlet pressure	outlet pressure	inlet gas density	outlet gas density	inlet gas velocity	outlet gas velocity	Reynolds number
	flow of gas	solids acceleration	flow of solids	elevation of gas	elevation of solids	Misc.	total pressure drop in section	C	Pa	Pa	kg/m^3	kg/m^3	m/s	m/s	
1	1,08	1509,02	122,12				1632,23	25,00	200000,00	198367,77	2,34	2,24	30,00	31,33	23987144,64
	1,08	1575,90	127,53				1704,51	25,00	198367,77	196663,26	2,24	2,22	31,33	31,60	23987144,64
	1,08	1589,56	128,64				1719,27	25,00	196663,26	194943,99	2,22	2,20	31,60	31,88	23987144,64
2	6,27	1603,57	791,09				2400,93	25,00	194943,99	192543,06	2,20	2,17	31,88	32,28	23987144,64
3	1,08	1623,57	131,39				1756,04	25,00	192543,06	190787,02	2,17	2,16	32,28	32,57	23987144,64
	1,08	1638,51	132,60				1772,19	25,00	190787,02	189014,82	2,16	2,14	32,57	32,88	23987144,64
	1,08	1653,88	133,84				1788,80	25,00	189014,82	187226,02	2,14	2,11	32,88	33,19	23987144,64
	1,08	1669,68	135,12				1805,88	25,00	187226,02	185420,14	2,11	2,09	33,19	33,52	23987144,64
	1,08	1685,94	136,44				1823,46	25,00	185420,14	183596,68	2,09	2,07	33,52	33,85	23987144,64
	1,08	1702,68	137,79				1841,56	25,00	183596,68	181755,13	2,07	2,05	33,85	34,19	23987144,64
	1,08	1719,94	139,19				1860,21	25,00	181755,13	179894,92	2,05	2,03	34,19	34,55	23987144,64
	1,08	1737,72	140,63				1879,43	25,00	179894,92	178015,49	2,03	2,01	34,55	34,91	23987144,64
	1,08	1756,07	142,11				1899,26	25,00	178015,49	176116,23	2,01	1,99	34,91	35,29	23987144,64

	1,08	651,51	143,65				796,24	25,00	176116,23	175319,99	1,99	1,98	35,29	35,45	23987144,64
	0,54	1783,07	72,15				1855,76	25,00	175319,99	173464,23	1,98	1,96	35,45	35,83	23987144,64
4	6,27	1802,14	889,05				2697,46	25,00	173464,23	170766,77	1,96	1,93	35,83	36,39	23987144,64
5	1,08	1830,61	148,14				1979,83	25,00	170766,77	168786,94	1,93	1,91	36,39	36,82	23987144,64
	1,08	1852,08	149,88				2003,05	25,00	168786,94	166783,89	1,91	1,88	36,82	37,26	23987144,64
	1,08	1874,32	151,68				2027,09	25,00	166783,89	164756,80	1,88	1,86	37,26	37,72	23987144,64
	1,08	1897,39	153,55				2052,02	25,00	164756,80	162704,79	1,86	1,84	37,72	38,20	23987144,64
	1,08	1921,32	155,49				2077,88	25,00	162704,79	160626,91	1,84	1,81	38,20	38,69	23987144,64
	1,08	1946,17	157,50				2104,75	25,00	160626,91	158522,16	1,81	1,79	38,69	39,20	23987144,64
	0,54	1972,01	79,79				2052,35	25,00	158522,16	156469,81	1,79	1,77	39,20	39,72	23987144,64
6	6,27	1997,88	985,61				2989,75	25,00	156469,81	153480,06	1,77	1,73	39,72	40,49	23987144,64
7	1,08	2036,79	164,83	34,01	38,08		2274,80	25,00	153480,06	151205,26	1,73	1,71	40,49	41,10	23987144,64
	1,08	2067,44	167,31	33,51	37,52		2306,86	25,00	151205,26	148898,40	1,71	1,68	41,10	41,74	23987144,64
	1,08	2099,47	169,90	33,00	36,95		2340,39	25,00	148898,40	146558,01	1,68	1,66	41,74	42,40	23987144,64
	1,08	2132,99	172,62	32,48	36,36		2375,53	25,00	146558,01	144182,47	1,66	1,63	42,40	43,10	23987144,64
	0,14	2168,14	21,93	3,99	4,47		2198,67	25,00	144182,47	141983,80	1,63	1,60	43,10	43,77	23987144,64
8	6,27	2201,71	1086,17				3294,15	25,00	141983,80	138689,66	1,60	1,57	43,77	44,81	23987144,64
9	1,08	2254,01	182,41				2437,49	25,00	138689,66	136252,16	1,57	1,54	44,81	45,61	23987144,64
	1,08	2294,33	185,67				2481,08	25,00	136252,16	133771,08	1,54	1,51	45,61	46,46	23987144,64
	1,08	2336,88	189,12				2527,08	25,00	133771,08	131244,00	1,51	1,48	46,46	47,35	23987144,64
	1,08	2381,88	192,76				2575,72	25,00	131244,00	128668,29	1,48	1,45	47,35	48,30	23987144,64
	1,08	2429,56	196,62				2627,26	25,00	128668,29	126041,03	1,45	1,42	48,30	49,31	23987144,64

	0,54	2480,20	100,36				2581,10	25,00	126041,03	123459,93	1,42	1,39	49,31	50,34	23987144,64
10	1,08	2532,05	1249,13				3782,27	25,00	123459,93	119677,66	1,39	1,35	50,34	51,93	23987144,64
11	0,54	2612,08	211,39	-26,52	-29,69		2767,79	25,00	119677,66	116909,87	1,35	1,32	51,93	53,16	23987144,64
	6,27	2673,92	81,15	-9,72	-10,88		2740,74	25,00	116909,87	114169,13	1,32	1,29	53,16	54,43	23987144,64
12	1,08	2738,11	1350,79				4089,97	25,00	114169,13	110079,16	1,29	1,24	54,43	56,46	23987144,64
13	0,41	2839,84	229,82				3070,07	25,00	110079,16	107009,09	1,24	1,21	56,46	58,08	23987144,64
	6,27	2921,31	236,41				3164,00	25,00	107009,09	103845,10	1,21	1,17	58,08	59,85	23987144,64
	1,08	3010,32	243,62				3255,02	25,00	103845,10	100590,08	1,17	1,14	59,85	61,78	23987144,64
	1,08	3107,73	251,50				3360,31	25,00	100590,08	97229,76	1,14	1,10	61,78	63,92	23987144,64
	1,08	3215,14	260,19				3476,41	25,00	97229,76	93753,35	1,10	1,06	63,92	66,29	23987144,64
14	1,08	3334,36	1644,93				4980,37	25,00	93753,35	88772,98	1,06	1,00	66,29	70,01	23987144,64
15	1,08	3521,42	284,98				3807,48	25,00	88772,98	84965,50	1,00	0,96	70,01	73,14	23987144,64
	6,27	3679,23	297,75				3983,24	25,00	84965,50	80982,26	0,96	0,91	73,14	76,74	23987144,64
	1,08	3860,19	312,39				4173,67	25,00	80982,26	76808,59	0,91	0,87	76,74	80,91	23987144,64
	1,08	4069,95	164,68				4235,72	25,00	76808,59	72572,88	0,87	0,82	80,91	85,63	23987144,64
Total pressure drop							**127427,12**			**127427,12**					**Turbulent flow: Re>4000**

	vertical sections
	initial conditions
	outlet conditions

M1 at solid conveying rate = 1 t/h and initial pressure = 3 bar

section number	pressure drop in each section, Pa							gas temperature	inlet pressure	outlet pressure	inlet gas density	outlet gas density	inlet gas velocity	outlet gas velocity	Reynolds number
	flow of gas	solids acceleration	flow of solids	elevation of gas	elevation of solids	Misc.	total pressure drop in section	C	Pa	Pa	kg/m^3	kg/m^3	m/s	m/s	
1	2,26	1106,62	65,67				1174,55	25,00	300000,00	298825,45	3,51	3,38	22,00	22,88	52779396,88
	2,26	1150,73	68,29				1221,29	25,00	298825,45	297604,16	3,38	3,36	22,88	22,97	52779396,88
	2,26	1155,45	68,57				1226,29	25,00	297604,16	296377,87	3,36	3,35	22,97	23,07	52779396,88
2	12,54	1160,23	419,74				1592,52	25,00	296377,87	294785,35	3,35	3,33	23,07	23,19	52779396,88
3	2,26	1166,50	69,23				1237,99	25,00	294785,35	293547,36	3,33	3,32	23,19	23,29	52779396,88
	2,26	1171,42	69,52				1243,20	25,00	293547,36	292304,16	3,32	3,30	23,29	23,39	52779396,88
	2,26	1176,40	69,82				1248,48	25,00	292304,16	291055,68	3,30	3,29	23,39	23,49	52779396,88
	2,26	1181,45	70,11				1253,83	25,00	291055,68	289801,85	3,29	3,27	23,49	23,59	52779396,88
	2,26	1186,56	70,42				1259,24	25,00	289801,85	288542,61	3,27	3,26	23,59	23,69	52779396,88
	2,26	1191,74	70,73				1264,73	25,00	288542,61	287277,88	3,26	3,25	23,69	23,80	52779396,88
	2,26	1196,99	71,04				1270,29	25,00	287277,88	286007,59	3,25	3,23	23,80	23,90	52779396,88
	2,26	1202,30	71,35				1275,92	25,00	286007,59	284731,68	3,23	3,22	23,90	24,01	52779396,88
	2,26	1207,69	71,67				1281,62	25,00	284731,68	283450,05	3,22	3,20	24,01	24,12	52779396,88
	2,26	651,51	72,00				725,77	25,00	283450,05	282724,28	3,20	3,19	24,12	24,18	52779396,88
	1,14	1216,27	36,09				1253,50	25,00	282724,28	281470,78	3,19	3,18	24,18	24,29	52779396,88
4	12,54	1221,68	441,97				1676,20	25,00	281470,78	279794,58	3,18	3,16	24,29	24,43	52779396,88
5	2,26	1229,00	72,94				1304,20	25,00	279794,58	278490,38	3,16	3,15	24,43	24,55	52779396,88
	2,26	1234,76	73,28				1310,30	25,00	278490,38	277180,09	3,15	3,13	24,55	24,66	52779396,88
	2,26	1240,59	73,62				1316,48	25,00	277180,09	275863,61	3,13	3,12	24,66	24,78	52779396,88
	2,26	1246,51	73,98				1322,75	25,00	275863,61	274540,85	3,12	3,10	24,78	24,90	52779396,88

	2,26	1252,52	74,33				1329,11	25,00	274540,85	273211,74	3,10	3,09	24,90	25,02	52779396,88
	2,26	1258,61	74,69				1335,57	25,00	273211,74	271876,17	3,09	3,07	25,02	25,14	52779396,88
	1,14	1264,80	37,53				1303,47	25,00	271876,17	270572,70	3,07	3,06	25,14	25,27	52779396,88
6	12,54	1270,89	459,77				1743,20	25,00	270572,70	268829,50	3,06	3,04	25,27	25,43	52779396,88
7	2,26	1279,13	75,91	59,58	60,64		1477,52	25,00	268829,50	267351,97	3,04	3,02	25,43	25,57	52779396,88
	2,26	1286,20	76,33	59,25	60,31		1484,35	25,00	267351,97	265867,63	3,02	3,00	25,57	25,71	52779396,88
	2,26	1293,38	76,76	58,92	59,97		1491,29	25,00	265867,63	264376,33	3,00	2,99	25,71	25,86	52779396,88
	2,26	1300,68	77,19	58,59	59,63		1498,35	25,00	264376,33	262877,98	2,99	2,97	25,86	26,01	52779396,88
	0,29	1308,09	9,70	7,28	7,41		1332,78	25,00	262877,98	261545,20	2,97	2,95	26,01	26,14	52779396,88
8	12,54	1314,76	475,64				1802,94	25,00	261545,20	259742,26	2,95	2,93	26,14	26,32	52779396,88
9	2,26	1323,88	78,57				1404,71	25,00	259742,26	258337,55	2,93	2,92	26,32	26,46	52779396,88
	2,26	1331,08	78,99				1412,34	25,00	258337,55	256925,21	2,92	2,90	26,46	26,61	52779396,88
	2,26	1338,40	79,43				1420,09	25,00	256925,21	255505,13	2,90	2,89	26,61	26,76	52779396,88
	2,26	1345,84	79,87				1427,97	25,00	255505,13	254077,16	2,89	2,87	26,76	26,91	52779396,88
	2,26	1353,40	80,32				1435,98	25,00	254077,16	252641,18	2,87	2,85	26,91	27,06	52779396,88
	1,14	1361,09	40,39				1402,62	25,00	252641,18	251238,56	2,85	2,84	27,06	27,21	52779396,88
10	2,26	1368,69	495,16				1866,11	25,00	251238,56	249372,45	2,84	2,82	27,21	27,41	52779396,88
11	1,14	1378,93	81,83	-55,27	-56,25		1350,39	25,00	249372,45	248022,05	2,82	2,80	27,41	27,56	52779396,88
	12,54	1386,44	30,85	-20,61	-20,98		1388,24	25,00	248022,05	246633,81	2,80	2,79	27,56	27,72	52779396,88
12	2,26	1394,24	504,40				1900,91	25,00	246633,81	244732,90	2,79	2,76	27,72	27,93	52779396,88
13	0,86	1405,07	83,39				1489,32	25,00	244732,90	243243,58	2,76	2,75	27,93	28,10	52779396,88
	12,54	1413,68	83,90				1510,11	25,00	243243,58	241733,46	2,75	2,73	28,10	28,28	52779396,88
	2,26	1422,51	84,42				1509,19	25,00	241733,46	240224,27	2,73	2,71	28,28	28,46	52779396,88
	2,26	1431,45	84,95				1518,66	25,00	240224,27	238705,61	2,71	2,70	28,46	28,64	52779396,88
	2,26	1440,55	85,49				1528,31	25,00	238705,61	237177,31	2,70	2,68	28,64	28,82	52779396,88
14	2,26	1449,83	524,51				1976,61	25,00	237177,31	235200,70	2,68	2,66	28,82	29,07	52779396,88
15	2,26	1462,02	86,77				1551,05	25,00	235200,70	233649,65	2,66	2,64	29,07	29,26	52779396,88
	12,54	1471,72	87,34				1571,61	25,00	233649,65	232078,05	2,64	2,62	29,26	29,46	52779396,88

	2,26	1481,69	87,93				1571,89	25,00	232078,05	230506,16	2,62	2,60	29,46	29,66	52779396,88
	2,26	1491,79	44,27				1538,32	25,00	230506,16	228967,84	2,60	2,59	29,66	29,86	52779396,88
Total pressure drop							**71032,16**			**71032,16**					**Turbulent flow: Re>4000**

M1 at solid conveying rate = 1 t/h and initial pressure = 4 bar

Section Number	pressure drop in each section, Pa							gas temperature	inlet pressure	outlet pressure	inlet gas density	outlet gas density	inlet gas velocity	outlet gas velocity	Reynolds number
	flow of gas	solids acceleration	flow of solids	elevation of gas	elevation of solids	Misc.	total pressure drop in section	C	Pa	Pa	kg/m3	kg/m3	m/s	m/s	
1	3,78	905,41	43,96				953,16	25,00	400000,00	399046,84	4,67	4,51	18,00	18,65	91461679,12
	3,78	938,05	45,55				987,38	25,00	399046,84	398059,46	4,51	4,50	18,65	18,70	91461679,12
	3,78	940,38	45,66				989,82	25,00	398059,46	397069,64	4,50	4,49	18,70	18,74	91461679,12
2	19,96	942,72	279,04				1241,73	25,00	397069,64	395827,91	4,49	4,47	18,74	18,80	91461679,12
3	3,78	945,68	45,92				995,38	25,00	395827,91	394832,53	4,47	4,46	18,80	18,85	91461679,12
	3,78	948,07	46,03				997,88	25,00	394832,53	393834,65	4,46	4,45	18,85	18,90	91461679,12
	3,78	950,47	46,15				1000,40	25,00	393834,65	392834,25	4,45	4,44	18,90	18,94	91461679,12
	3,78	952,89	46,27				1002,94	25,00	392834,25	391831,31	4,44	4,43	18,94	18,99	91461679,12
	3,78	955,33	46,39				1005,49	25,00	391831,31	390825,81	4,43	4,41	18,99	19,04	91461679,12
	3,78	957,78	46,51				1008,07	25,00	390825,81	389817,74	4,41	4,40	19,04	19,09	91461679,12

	3,78	960,26	46,63				1010,67	25,00	389817,74	388807,07	4,40	4,39	19,09	19,14	91461679,12
	3,78	962,76	46,75				1013,29	25,00	388807,07	387793,79	4,39	4,38	19,14	19,19	91461679,12
	3,78	965,27	46,87				1015,92	25,00	387793,79	386777,86	4,38	4,37	19,19	19,24	91461679,12
	3,78	651,51	46,99				702,29	25,00	386777,86	386075,58	4,37	4,36	19,24	19,28	91461679,12
	1,92	969,57	23,54				995,03	25,00	386075,58	385080,54	4,36	4,35	19,28	19,33	91461679,12
4	19,96	972,07	287,73				1279,77	25,00	385080,54	383800,77	4,35	4,34	19,33	19,39	91461679,12
5	3,78	975,32	47,36				1026,45	25,00	383800,77	382774,32	4,34	4,32	19,39	19,44	91461679,12
	3,78	977,93	47,48				1029,20	25,00	382774,32	381745,12	4,32	4,31	19,44	19,49	91461679,12
	3,78	980,57	47,61				1031,96	25,00	381745,12	380713,16	4,31	4,30	19,49	19,55	91461679,12
	3,78	983,23	47,74				1034,75	25,00	380713,16	379678,41	4,30	4,29	19,55	19,60	91461679,12
	3,78	985,91	47,87				1037,56	25,00	379678,41	378640,86	4,29	4,28	19,60	19,65	91461679,12
	3,78	988,61	48,00				1040,39	25,00	378640,86	377600,47	4,28	4,27	19,65	19,71	91461679,12
	1,92	991,33	24,07				1017,32	25,00	377600,47	376583,14	4,27	4,25	19,71	19,76	91461679,12
6	19,96	994,01	294,22				1308,20	25,00	376583,14	375274,95	4,25	4,24	19,76	19,83	91461679,12
7	3,78	997,47	48,43	83,17	77,76		1210,62	25,00	375274,95	374064,33	4,24	4,23	19,83	19,89	91461679,12
	3,78	1000,70	48,59	82,90	77,51		1213,49	25,00	374064,33	372850,84	4,23	4,21	19,89	19,96	91461679,12
	3,78	1003,96	48,75	82,63	77,26		1216,38	25,00	372850,84	371634,46	4,21	4,20	19,96	20,02	91461679,12
	3,78	1007,25	48,91	82,36	77,01		1219,30	25,00	371634,46	370415,16	4,20	4,18	20,02	20,09	91461679,12
	0,49	1010,56	6,13	10,26	9,59		1037,04	25,00	370415,16	369378,12	4,18	4,17	20,09	20,15	91461679,12
8	19,96	1013,40	299,96				1333,32	25,00	369378,12	368044,79	4,17	4,16	20,15	20,22	91461679,12
9	3,78	1017,07	49,38				1070,23	25,00	368044,79	366974,56	4,16	4,15	20,22	20,28	91461679,12
	3,78	1020,04	49,53				1073,35	25,00	366974,56	365901,22	4,15	4,13	20,28	20,34	91461679,12

	3,78	1023,03	49,67				1076,48	25,00	365901,22	364824,73	4,13	4,12	20,34	20,40	91461679,12
	3,78	1026,05	49,82				1079,65	25,00	364824,73	363745,08	4,12	4,11	20,40	20,46	91461679,12
	3,78	1029,09	49,97				1082,84	25,00	363745,08	362662,24	4,11	4,10	20,46	20,52	91461679,12
	1,92	1032,16	25,06				1059,15	25,00	362662,24	361603,10	4,10	4,08	20,52	20,58	91461679,12
10	3,78	1035,19	306,41				1345,38	25,00	361603,10	360257,72	4,08	4,07	20,58	20,66	91461679,12
11	1,92	1039,05	50,45	-79,84	-74,65		936,94	25,00	360257,72	359320,78	4,07	4,06	20,66	20,71	91461679,12
	19,96	1041,76	18,97	-29,86	-27,92		1022,91	25,00	359320,78	358297,86	4,06	4,05	20,71	20,77	91461679,12
12	3,78	1044,74	309,24				1357,76	25,00	358297,86	356940,11	4,05	4,03	20,77	20,85	91461679,12
13	1,45	1048,71	50,92				1101,08	25,00	356940,11	355839,02	4,03	4,02	20,85	20,91	91461679,12
	19,96	1051,96	51,08				1123,00	25,00	355839,02	354716,03	4,02	4,01	20,91	20,98	91461679,12
	3,78	1055,29	51,24				1110,31	25,00	354716,03	353605,72	4,01	3,99	20,98	21,05	91461679,12
	3,78	1058,60	51,40				1113,78	25,00	353605,72	352491,94	3,99	3,98	21,05	21,11	91461679,12
	3,78	1061,95	51,56				1117,29	25,00	352491,94	351374,65	3,98	3,97	21,11	21,18	91461679,12
14	3,78	1065,32	315,33				1384,43	25,00	351374,65	349990,21	3,97	3,95	21,18	21,26	91461679,12
15	3,78	1069,54	51,93				1125,25	25,00	349990,21	348864,96	3,95	3,94	21,26	21,33	91461679,12
	19,96	1072,99	52,10				1145,05	25,00	348864,96	347719,91	3,94	3,93	21,33	21,40	91461679,12
	3,78	1076,52	52,27				1132,57	25,00	347719,91	346587,34	3,93	3,91	21,40	21,47	91461679,12
	3,78	1080,04	26,22				1110,04	25,00	346587,34	345477,30	3,91	3,90	21,47	21,54	91461679,12
Total pressure drop							**54522,70**			**54522,70**					**Turbulent flow: Re>40000**

Appendix E

Python program

```
import pandas as pd
import os
import sys
import numpy as np
import matplotlib.pyplot as plt
import seaborn as sns
import utilities as u

#User inputs
ExpName = "M2000C75_06.11.2022" #Enter folder name
tRange = [90,120]  #Enter minimum and maximum time for averaging

#Raw data processing - Contains time between 90 - 120 sec for each
df = u.arrangedata(ExpName, tRange)
df.to_excel("Results//Raw_{}.xlsx".format(ExpName),index=None)

#Statisitcally processed data - Contains mean and standard deviation of the
raw data
df_stat = u.statisticalAnalysis(df)
df_stat.to_excel("Results//Statistical_{}.xlsx".format(ExpName),index=None)

#Plot to visualize
plt.figure()
plt.grid(True)
plt.plot(df_stat["Gas velocity [Nm/s]"], df_stat["dP (Mean)"],label=r"Mean")
plt.fill_between(df_stat["Gas velocity [Nm/s]"], df_stat["dP (Minimum)"],
df_stat["dP (Maximum)"], alpha=0.2,label=r"Mean")
plt.xlabel("Gas velocity [Nm/s]")
plt.ylabel("Pressure drop [mbar]")
```